Chapter 9

Rock Avalanches onto Glaciers

Philip Deline [1], **Kenneth Hewitt** [2], **Natalya Reznichenko** [3] **and Dan Shugar** [4]

[1] *EDYTEM Lab, Université de Savoie, CNRS, Le Bourget-du-Lac, France,* [2] *Geography and Environmental Studies, Wilfrid Laurier University, Waterloo, Ontario, Canada,* [3] *Department of Geography, Durham University, Durham, UK,* [4] *Department of Geography, University of Victoria, British Columbia, Canada*

ABSTRACT

The chapter looks mainly at massive rock slope failures that generate high-speed, long-runout rock avalanches onto glaciers in high mountains, from subpolar through tropical latitudes. Drastic modifications of mountain landscapes and destructive impacts occur, and initiate other, longer-term hazards. Worst-case calamities are where mass flows continue into inhabited areas below the glaciers. Travel over glaciers can change landslide dynamics and amplify the speed and length of runout. Conversely, landslide material deposited onto ice modifies glacier behavior, protecting ice from ablation, usually causing advances and hugely increasing glacier sediment delivery. Hitherto, recognition of the risks associated with these processes has been compromised by observational difficulties and theoretical disagreements, lack of evidence in many regions and widespread misclassification of rock avalanche deposits as moraines. The latter has also compromised glacial sequences and risk scenarios. We emphasize the need for improved understanding of processes and diagnostics, as prelude to risk assessments, including the roles of earthquakes and climate change.

9.1 INTRODUCTION

Landslide processes that affect glaciers range from small rockfalls and snow avalanches to massive rock slope failures and deep-seated gravitational creep[1]. The more frequent, smaller events may have a significant role as they affect virtually all mountain glaciers seasonally every year. This is reflected in the debris-covered ablation zones common in high mountain glaciers, and substantial delivery of coarse, angular debris to glacier margins. However, though infrequent, large volume and long-runout events can have powerful influences on glacier

[1] Photos by authors unless otherwise stated

Landslide Hazards, Risks, and Disasters. http://dx.doi.org/10.1016/B978-0-12-396452-6.00009-4

dynamics, sediment assemblages, and landform development (Hewitt et al., 2011b; Reznichenko et al., 2012; Shugar et al., 2012). Travel over glaciers results in greater speed and reach of long-runout events than is the case with landslides that travel over other substrates. The mobility of the landslide debris is affected by travel over ice and by incorporation of snow, ice, meltwater, or wet sediment from the glacier (Evans and Clague, 1988). This may also result in changes of character and dynamics of mass flows. Rock avalanches may be transformed into debris avalanches—large debris-flow-like or complex mass flow events.

The chapter will focus mainly on massive rock slope failures that result in rock avalanches onto alpine glaciers in high mountains. Rock avalanches, involving the extremely rapid, flowlike movement of crushed and pulverized rock material, are among the few surface processes that can cause large, almost instantaneous modifications of mountain landscapes. Massive rock slope failures produce deep head-scarps, leaving a strong imprint on landforms in their travel zones and huge areas buried in debris. They are characterized by large volumes, generally not less than 1 Mm^3. Some are "megaslides" exceeding 1 km^3. In high mountains their motion involves great vertical falls (>1,000 m), long horizontal travel distances (>5 km), and high velocities (>25 m/s).

These landslides pose both direct and indirect hazards to society. No one is likely to survive in the path of a rock avalanche. However, they are sufficiently rare, and the exposure of humans on glaciers is so limited that few fatal cases are known. The greatest risks and worst calamities associated with these events are where runout continues below the glaciers into areas that have human settlements and infrastructure. A number of recent calamitous examples have occurred in the Andes and Inner Asian high mountains (Table 9.1). Indirect or secondary hazards can arise from the impact of the landslide on glacier activity, notably if it results in thickening and sudden advance, or where the landslide mass impounds meltwater along the glacier margins or streams in ice-free valleys below. The inundation of land or outburst floods from such impoundments can be serious threats.

We examine the conditions likely to create rock slope instability and trigger catastrophic failures, landslide behavior during travel over and beyond the glaciers, and the resulting depositional and erosional legacies. An outstanding question is the extent to which global climate change may increase these hazards or alter their geographical patterns. This may follow from greater weather extremes that trigger events, or degrading of mountain permafrost so as to destabilize rockwalls (Davies et al., 2001; Haeberli et al., 2002; Fischer et al., 2006; Huggel, 2008). Meanwhile, risks will inevitably increase because of greater human presence and activity in the mountains. However, these require risk assessments using probabilities based on evidence of older or prehistoric events, even though they occurred when settlements were absent or much more dispersed.

Full appreciation of the topic and the hazards involved has been compromised by three main factors: (1) difficulty in identifying deposits in remote mountain ranges before they are covered by snow, heavily modified, and

TABLE 9.1 Statistics of Documented Rock Avalanches onto Glacier with a Rock Volume >1 Mm^3 since 1950

Rock Avalanche (Country Codes: ISO 3166-1 Alpha-3)	Year	V_R[1] (Mm^3)	V_I[2] (Mm^3)	H (km)	L (km)	μ[3]	L_e[4] (km)	A[5] (km^2)	Th[6] (m)	V_{i+s}[7] (Mm^3)	P_{Gl}[8] (km)	P_{Marg}[9] (km)	Z[10] (m)	References
Becca di Luseney (*Valpelline, ITA*)	1952	1.0	0.0	1.65	4.00	0.41	1.35	?	?	?	0.30	0.00	3,265	Dutto and Mortara (1991)
Tim Williams Glacier (*Coast Mts, CAN*)	1956	3.0	?	0.94	3.70	0.25	2.20	?	?	?	?	0.00	?	Evans and Clague (1999)
Pandemonium Creek (*Coast Mts, CAN*)	1959	5.5	0.0	2.00	8.60	0.23	5.35	1.50	?	50%	1.39	0.00	2,600	Evans and Clague (1999), Evans and Clague (1988), Schneider et al. (2011b)
Iliamna Red Glacier (*Chigmit Range, USA*)	1960	*<2.0	?	1.47	5.50	0.27	3.15	?	?	60%	5.10	0.00	2,125	Schneider et al. (2011b)
Nevados Huascarán (*Cordillera Bl., PER*)	1962	1.0	2.0	4.08	18.10	0.23	11.50	?	?	15.6	2.40	3.50	6,654	Schneider et al. (2011b), Plafker and Ericksen (1978), Evans et al. (2009a)
Little Tahoma Peak[12] (*Mount Rainer, USA*)	1963	10.7	0.0	1.88	7.25	0.26	4.25	5.00	1–20	20%	4.33	13.55	3,230	Crandell and Fahnestock (1965), Fahnestock (1978)
Schwan Glacier 1 (*Chugach Mts, USA*)[11]	1964	27.0	?	1.45	6.00	0.24	3.65	9.00	?	?	5.35	0.00	2,180	Evans and Clague (1988), Post (1967)
Sherman Glacier (*Chugach Mts, USA*)[11]	1964	10.1	2.0	1.16	6.00	0.19	4.15	8.25	1.6	>2.0	5.13	3.60	1,310	Post (1967), McSaveney (1978)

Continued

TABLE 9.1 Statistics of Documented Rock Avalanches onto Glacier with a Rock Volume >1 Mm^3 since 1950—cont'd

Rock Avalanche (Country Codes: ISO 3166-1 Alpha-3)	Year	V_R[1] (Mm^3)	V_I[2] (Mm^3)	H (km)	L (km)	μ[3]	L_e[4] (km)	A[5] (km^2)	Th[6] (m)	V_{i+s}[7] (Mm^3)	P_{GI}[8] (km)	P_{Marg}[9] (km)	Z[10] (m)	References
Sioux Glacier 1 (*Chugach Mts, USA*)[11]	1964	7.0	?	1.35	4.50	0.30	2.30	3.10	2.0	2.3	3.60	0.70	1,525	Post (1967), Reid (1969)
Steller Glacier 1 (*Chugach Mts, USA*)[11]	1964	20.0	?	1.15	6.70	0.17	4.85	7.50	?	?	5.80	0.63	2,700	Evans and Clague (1988), Post (1967)
Allen Glacier 4 (*Chugach Mts, USA*)	?1965	23.0	?	1.23	7.70	0.16	5.75	7.50	?	?	7.03	0.45	1,925	Evans and Clague (1988), Post (1967)
Fairweather Glacier (*Chugach Mts, USA*)	?1965	26.0	?	3.35	10.50	0.32	5.10	8.50	?	?	7.90	0.00	4,050	Evans and Clague (1988), Post (1967)
Steinsholtsjokull Glacier (*Eyjafjallajökull, ISL*)	1967	15.0	<6.00	0.32	5.00	0.06	4.50	0.28	2–5	>20.0	1.20	1.10	710	Kjartansson (1967)
Nevados Huascarán (*Cordillera Bl., PER*)[11]	1970	6.5	1.0	3.92	18.20	0.22	11.90	22.00	?	58.2	2.40	0.00	6,654	Plafker and Ericksen (1978), Evans et al. (2009a)
Winthrop Glacier (*Mount Rainier, USA*)	1974	?	0.0	1.39	2.70	0.51	0.45	0.75	?	?	2.25	0.00	3,705	Scott and Vallance (1995)
Devastation Glacier (*Coast Mts, CAN*)	1975	13.0		1.22	7.00	0.17	5.05	?	?	?	2.50	0.00	2,010	Evans and Clague (1999), Evans and Clague (1988)
Iliamna Red Glacier (*Chigmit Range, USA*)	1978	*6.8	?	1.78	7.70	0.23	4.85	?	?	60%	7.00	?	2,310	Schneider et al. (2011b)

Ama Dablam (*Khumbu Himal, NPL*)	1979	>1.0	0.0	1.40	3.00	0.47	0.75	>0.75	?	?	2.10	1.80	5,600	Selby (1993)
Iliamna Red Glacier (*Chigmit Range, USA*)	1980	*11.2	?	1.68	7.80	0.22	5.10	?	?	60%	7.35	0.07[13]	2,193	Schneider et al. (2011b)
W Fork Robertson Glacier (*Alaska Range, USA*)	1981	2.2	?	0.70	3.50	0.20	2.35	1.50	2–5	?	3.00	0.14	2,100	Herreid et al. (2010)
Marvine Glacier (*St. Elias Mountains, USA*)	1983	1	?	0.86	3.15	0.27	1.75	?		70%	2.05	0.27	1,650	Schneider et al. (2011b)
Glacier de Bualtar 1 (*Karakorum, PAK*)	1986	10.0	0.0	1.49	4.80	0.31	2.40	4.10	2.5	?	3.25	0.00	4,450	Hewitt (1988)
Glacier de Bualtar 2 (*Karakorum, PAK*)	1986	7.0	0.0	1.43	3.70	0.39	1.40	3.30	2.1	?	2.15	0.00	4,450	Hewitt (1988)
Glacier de Bualtar 3 (*Karakorum, PAK*)	1986	3.0	0.0	1.30	2.40	0.54	0.30	1.20	2.5	?	0.85	0.50	4,450	Hewitt (1988)
Mount Meager (*Coast Mountains, CAN*)	1986	0.5–1.0	0.0	1.34	3.68	0.36	1.50	?	?	?	?	0.00	2,400	Evans and Clague (1988)
North Creek (*Coast Mountains, CAN*)	1986	1.0–2.0	0.0	0.75	2.85	0.26	1.65	?	?	?	1.00	0.75	1,980	Evans and Clague (1988)
Aroaki/Mount Cook (*Southern Alps, NZL*)	1991	9.4–14.2	0.4–0.6	2.72	7.50	0.36	3.10	7.00	2–10	>30.0	6.66	0.60	3,764	McSaveney (2002)
Mount Fletcher 1 (*Southern Alps, NZL*)	1992	>7.8	4%	1.44	3.80	0.38	1.00	1.75	?	?	2.29	1.20	2,450	McSaveney (1993)
Mount Fletcher 2 (*Southern Alps, NZL*)	1992	>5.0	0.0	1.44	3.80	0.38	1.45	1.75	?	?	2.36	0.50	2,450	McSaveney (1993)

Continued

TABLE 9.1 Statistics of Documented Rock Avalanches onto Glacier with a Rock Volume >1 Mm^3 since 1950—cont'd

Rock Avalanche (Country Codes: ISO 3166-1 Alpha-3)	Year	V_R[1] (Mm^3)	V_I[2] (Mm^3)	H (km)	L (km)	μ[3]	L_e[4] (km)	A[5] (km^2)	Th[6] (m)	V_{i+s}[7] (Mm^3)	P_{Gl}[8] (km)	P_{Marg}[9] (km)	Z[10] (m)	References
Winthrop Glacier (*Mount Rainier, USA*)	1992	?	0.0	1.30	2.45	0.53	0.35	0.45	?	?	1.90	0.55	3,780	Scott and Vallance (1995)
Kshwan Glacier (*Coast Mountains, CAN*)	?1992	3.2	0.0	0.79	2.25	0.35	1.00	0.68	5	–	1.42	16.3	1,750	Evans and Clague (1999), Mauthner (1996)
Iliamna Red Glacier (*Chigmit Range, USA*)	1994	*10.2	?	1.80	10.0	0.18	7.10	?	?	60%	9.50	0.00	2,230	Schneider et al. (2011b)
Mount Munday (*Coast Mountains, CAN*)	1997	3.2	0.0	0.88	4.70	0.19	3.30	2.20	1.5	?	>3.50	0.00	3,000	Evans and Clague (1999), Evans and Clague (1998)
Brenva Glacier (*Mont Blanc massif, ITA*)	1997	2.0	0.0	2.33	5.75	0.40	0.20	?	1	>4.5	5.40	0.00	3,725	Deline (2001, 2009)
Iliamna Red Glacier (*Chigmit Range, USA*)	1997	*8.4	?	1.71	7.70	0.22	4.95	?	?	60%	7.10	0.00	2,230	Schneider et al. (2011b)
Howson Glacier 2 (*Coast Mountains, CAN*)	1999	0.9	?	1.30	2.70	0.48	0.60	?	?	?	1.50	0.00	?	Schwab (2002)
Iliamna Red Glacier (*Chigmit Range, USA*)	2000	*9.0	?	1.83	8.90	0.21	5.95	?	?	60%	8.40	0.00	2,310	Schneider et al. (2011b)
Tsar Mountain (*Rockies Mountains, CAN*)	2000	1.6	?	0.61	2.25	0.27	1.25	?	?	40%	1.70	0.00	2,778	Jiskoot (2011a)

Kolka-Karmadon (*Caucasus, RUS*)	2002	10–14.0	8.5–13	2.05	19.40	0.11	16.10	?	?	90.0	3.10	0.00	3,368	Schneider et al. (2011b), Huggel et al. (2005)
McGinnis Peak Glacier N (*Alaska Range, USA*)[11]	2002	18.4	?	1.65	11.00	0.15	8.45	10.21	2	2.0	10.50	0.00	2,740	Jibson et al. (2006)
McGinnis Peak Glacier S (*Alaska Range, USA*)[11]	2002	11.4	?	1.80	11.50	0.16	8.60	5.71	2	?	10.70	2.30	2,770	Jibson et al. (2006)
Black Rapids Glacier E (*Alaska Range, USA*)[11]	2002	9.3–14.0	?	0.98	4.10	0.24	2.50	4.64	2–3	?	3.60	0.00	2,130	Jibson et al. (2006), Shugar and Clague (2011)
Black Rapids Glacier M (*Alaska Range, USA*)[11]	2002	7.7–11.6	?	0.80	5.60	0.14	4.30	4.55	2–3	?	3.20	0.00	2,050	Jibson et al. (2006), Shugar and Clague (2011)
Black Rapids Glacier W (*Alaska Range, USA*)[11]	2002	4.9–7.4	?	0.73	3.40	0.21	2.20	3.24	2–3	?	2.20	0.00	2,070	Jibson et al. (2006), Shugar and Clague (2011)
West Fork Glacier N (*Alaska range, USA*)[11]	2002	4.1	?	0.76	3.30	0.23	2.10	1.37	3	?		0.85	1,980	Jibson et al. (2006)
West Fork Glacier S (*Alaska Range, USA*)[11]	2002	4.4	?	0.90	4.10	0.22	2.65	1.47	3	?		10.85	2,070	Jibson et al. (2006)
Iliamna Red Glacier (*Chigmit Range, USA*)	2003	*6.0	6.0–14	1.98	8.60	0.23	5.40	4.00	1–2	60%	8.00	0.00	2,256	Huggel et al. (2007)
Iliamna Umbrella Glacier (*Chigmit Range, USA*)	2004	*2.0	?	1.76	6.05	0.29	3.20	?	?	50%	5.55	0.00	2,406	Schneider et al. (2011b)
Punta Thurwieser (*Ortles-Cevedale, ITA*)	2004	2.5	0.0	1.30	2.70	0.48	0.60	?	?	10%	0.40	0.00	3,570	Schneider et al. (2011b), Sossio et al. (2008), Pirulli (2009)
Mount Steller (*St Elias Mountains, USA*)	2005	>40.0	>3.0	2.43	9.00	0.27	5.10	?	?	0.36	8.64	0.00	3,100	Huggel et al. (2008)

Continued

TABLE 9.1 Statistics of Documented Rock Avalanches onto Glacier with a Rock Volume >1 Mm^3 since 1950—cont'd

Rock Avalanche (Country Codes: ISO 3166-1 Alpha-3)	Year	V_R[1] (Mm^3)	V_I[2] (Mm^3)	H (km)	L (km)	μ[3]	L_e[4] (km)	A[5] (km^2)	Th[6] (m)	V_{i+s}[7] (Mm^3)	P_{Gl}[8] (km)	P_{Marg}[9] (km)	Z[10] (m)	References
Mount Steele (*St Elias Mountains, CAN*)	2007	27.5–80.5		2.16	5.80	0.32	2.30	5.28	4–22	30%	4.05	0.00	4,650	Lipovski et al. (2008)
Morsárjökull (*Vatnajökull Ice Cap, ISL*)	2007	4.0	0.0	0.66	1.40	0.47	0.35	0.72	5.5	–	1.70	0.00	950	Decaulne et al. (2010)
Mount Miller (*St Elias Mountains, USA*)	2008	*22.0	?	0.91	4.50	0.20	3.05	?	?	?	3.65	3.50	2,200	Schneider et al. (2011b)
Mount Meager (*Coast Mts, CAN*)	2010	48.5	<0.2	2.18	12.70	0.17	9.20	9.00	?	<1%	<0.50	>12.0	2,554	Guthrie et al. (2012)
Lituya Mountain (*Coast Mts, USA*)	2012	>20.0		2.50	9.00	0.28	4.95	7–8.00	?	?	6.50	0.00	3,030	Geertsema (2012)
Mount Dixon (*Southern Alps, NZL*)	2013	1.5?	?	0.85	2.80	0.30	1.45	0.75	1–2	?	2.55	3.60	2,950	http://blogs.agu.org/landslideblog

Name: Catastrophic glacier multiphase event (*sensu* Petrakov et al., 2008).
? – Unknown data.
[1]*Detached (*: deposited) rock volume.*
[2]*Detached ice volume.*
[3]$\mu = H/L$.
[4]*Excessive travel distance* $L_e = L - H/\tan 32$.
[5]*Surface area of the deposit.*
[6]*Mean thickness of final rock deposit (___: ice and rock deposit).*
[7]*Ice and snow volume of the deposit (or % of the total (rock + ice) deposited volume).*
[8]*Path onto glacier surface.*
[9]*Path on margins (outside of the glacier).*
[10]*Maximal elevation of the scar.*
[11]*Rock avalanche triggered by earthquake.*
[12]*Seven successive rock collapses (data: main collapse).*
[13]*Run-up on moraine proximal side.*

dispersed by glacier transport; (2) widespread misclassifying of rock avalanche deposits as moraines (Heim, 1932; Porter and Orombelli, 1980; Hewitt, 1999; Prager et al., 2009; McColl and Davies, 2011); and (3) recognition that some moraines result from supraglacial rock avalanche deposits rather than from climatic variation (Reznichenko et al., 2012). Rock avalanche deposits need to be distinguished from the many other coarse, poorly-sorted, or unsorted materials in mountain glacier environments. The problem is further complicated where rock avalanches descend over surge-type glaciers, as reported in the Alaska–Yukon ranges, Argentinian Andes, Caucasus, Pamirs, and Karakoram. In such cases they become involved in the already complex issues of interpreting surge-induced glacial deposits (Sharp, 1988; Evans and Rea, 2003). Further, inventories of rock avalanches on glaciers have been hindered by difficulties associated with observing them. Their unpredictability and frequent location in remote mountains have made observations rare. Their known numbers are certainly underestimates.

The first section of the chapter is dedicated to the processes that are involved in the detachment, the displacement, and the deposition of the rock avalanches onto and beyond glaciers, and the subsequent transformation of the deposits. Then the interactions between rock avalanches and glaciers are explored in terms of high mobility of the landslide material, debris supply to glaciers and changes in glacier dynamics, and character of the resulting moraine complexes. Finally, three regional and local case studies are presented from the Karakoram Himalaya, New Zealand Alps, and Argentinian Andes.

9.2 PROCESSES

9.2.1 Detachment Zone and Conditions

Several sets of factors affect the occurrence of a landslide: inherent factors (e.g., rock structure, slope form), preparatory factors (e.g., weathering, debuttressing, climate change), triggering factors (e.g., earthquake, rainstorm), and factors that may affect mobility (e.g., glacier surface) (Pacione, 1999). Here we consider two categories of causal factors in a rock failure: preparatory factors and triggers (see also Chapter 2 in this volume). The former operate over a lengthy period to reduce the stability of the slope, while the latter are external stimuli, operating over a short period, which rapidly increase the total stress on a slope or reduce the strength of the slope, causing it to fail (Lee and Jones, 2004). In some cases, no identifiable trigger is evident. In these cases it seems the stability of the slope has deteriorated over time, e.g., stress corrosion to reach a spontaneous failure threshold (Eberhardt et al., 2004), or the actual trigger factor remained unidentified (e.g., rock avalanches described by McSaveney (2002), Lipovsky et al. (2008)).

9.2.1.1 Preparatory Factors

Lithology and structure are two well-known control factors for rockfall and massive rock slope failure. Shear zones with crushed rock (e.g.,

mylonitoschists in the Mont Blanc massif; the active Raikot-Sassi and Stak fault systems of the Nanga Parbat-Haramosh massif, NW Himalaya) are particularly prone to rockfall and rock avalanching.

These conditions may combine with paraglacial dynamics; conditions that follow from former glacial action and deglaciation. During a paraglacial period, three processes can act to destabilize rock slopes:

1. glacial overdeepening may increase the preglacial rock slope stress and cause possible slope instability (McColl, 2012); due to uplift and glacier erosion, relative relief of mountainsides in Himalaya, Rockies, or European Alps can exceed 2,500−3,000 m, and with slope angles >45°;
2. shrinkage and downwasting of glaciers results in glacial debuttressing (Cossart et al., 2008), i.e., the loss of slope support provided by glacial ice; although whether this can prevent a failure being triggered, or simply constrains the movement of the failed mass, is unclear (McColl and Davies, 2013);
3. the removal of glacier ice can generate near-surface rock fractures parallel to the slope; this stress-release fracturing weakens the rock and prepares its instability (McColl, 2012).

The 1992 rock avalanches on Mount Fletcher (Southern Alps, NZ) illustrate these processes. They combine a 250-m post-Little Ice Age (LIA) debuttressed foot of a 1,000-m-high, 57° slope angle, mountain side, with near-surface fractures parallel to the slope, corresponding to the detachment zones of the rock avalanches (McSaveney, 1993). Generally, there is a strong association in the central Southern Alps of recent slope failures with glacial shrinkage over the past 100−150 years (Allen et al., 2011).

Moreover, glacier surfaces lowered by tens to hundreds of meters, especially in the ablation zone, may have an effect on rock temperature regime, as identified for >300 m in the frontal area of Grosser Aletschgletscher since the LIA termination, and for 250 m at Black Rapids Glacier since 1949 (Shugar et al., 2010). Once close to 0 °C, the rock temperature of the deglaciated rockwalls responds to local air temperature, depending on orientation, so that freeze-front propagation can fracture the rock (Wegmann et al., 1998; Nagai et al., 2013). At lower elevations, slope dewatering due to glacier retreat tends to destabilize the foot slope because of the reorientation of its stress field (Haeberli et al., 1997; McColl et al., 2010)—although it also reduces the pore-water pressure. On the other hand, surface lowering of glaciers and melting of ice aprons and small hanging glaciers can lead to permafrost development in rock slopes previously covered by ice (Haeberli et al., 1997; Fischer et al., 2006).

Permafrost degradation due to climate warming generates physical changes in the formerly frozen rock mass. Interstitial ice can melt, whereas heat advection and hydrostatic pressure can be produced at depth in a densely fractured rock mass by circulation of water from the melting of surface snow cover and/or cleft ice (Hasler et al., 2011; Wegmann et al., 1998). The upward

warming of the permafrost base in high-elevation rockwalls combined with a frozen rock surface layer can produce high groundwater pressure (Wegmann et al., 1998). Deep degradation of rock permafrost may be delayed by decades, centuries, or millennia (Gruber and Haeberli, 2007). The 22 rock failures observed in the central region of the NZ Southern Alps since the mid-twentieth century have mainly affected rockwalls with warm permafrost, i.e., whose temperature is in the range −2 to 0 °C, and nearly all of the recent rock avalanches were associated with glaciers (Allen et al., 2011).

Because the majority of rock avalanches have occurred in glaciated mountain ranges that are tectonically active (Figure 9.1), or impacted by the removal of ice caps (McColl et al., 2012), seismicity can also lead to the gradual, or intermittent destabilization of susceptible slopes, acting as a preparatory as well as a common triggering factor. Repeated seismic shaking weakens a rock mass until it reaches the threshold when a rock avalanche may be triggered by the next seismic event or by other causes (Voight, 1978; Eisbacher and Clague, 1984).

9.2.1.2 *Triggering Factors*

Freeze-thaw action is conditioned by the temperature fluctuations around 0 °C and may occur at depth during or following permafrost degradation. Volumetric expansion of ice in the slope generally widens existing fractures and prepares the rock for failure (Gruber and Haeberli, 2007; Murton and Matsuoka, 2008). Whereas this freeze-thaw action was observed and empirically proven to cause smaller mass failure events such as rockfalls (Gruber et al., 2004; Matsuoka and Murton, 2008), it is uncertain whether it could lead to massive rock slope failures and rock avalanches (Whalley, 1984; Davies et al., 2001).

Strong ground shaking during earthquakes has triggered landslides in diverse topographic and geologic settings. In the Chugach Mountains of south-central Alaska, Uhlmann et al. (2013) estimate that half of the supraglacial rock avalanches and c. 73 percent of the RA volume emplaced onto glaciers were triggered by coseismic shaking. The March 27, 1964 M 9.2 earthquake located on the south coast of Alaska triggered 50 rock avalanches onto glaciers with a total deposit area $>0.5 \times 10^6$ m^2 (Post, 1967), whereas the 1979 St Elias earthquake triggered at least three rock avalanches onto glaciers in northern British Columbia (Evans and Clague, 1999). As suggested by a study of some 50 large coseismic landslides worldwide (Keefer, 1984), slopes affected generally have a relative relief >150 m (median: 500 m) and a slope angle >25° (median 40°). Keefer (2002) also established a correlation between earthquake magnitude and landslide-affected area for a large sample of events. However, the area affected by coseismic landslides varies greatly from event to event. The 1964 M 9.2 earthquake involved 269,000 km^2; the 2002 Alaskan M 7.9 earthquake only 10,000 km^2, much less than expected (Jibson et al., 2006).

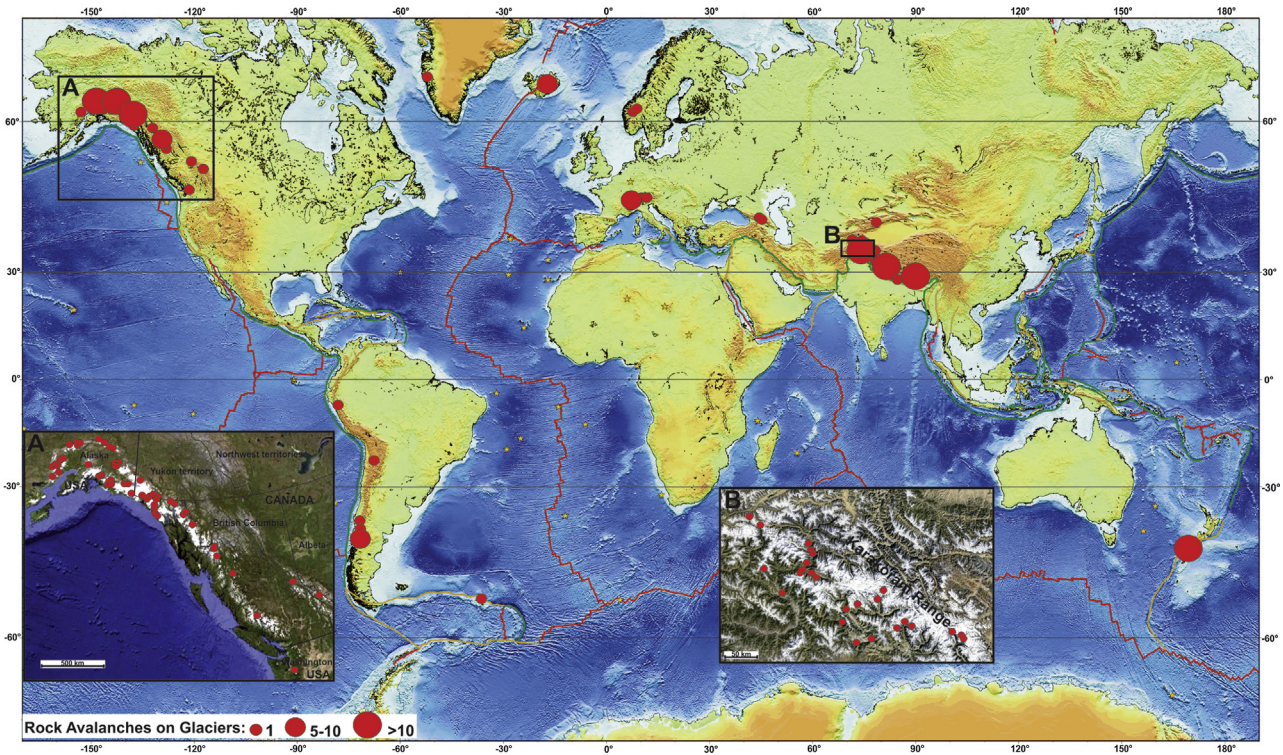

FIGURE 9.1 Distribution of main documented rock avalanches onto glacier worldwide. A: Northwestern North America; B: Karakoram Range.

The dimensions of the seismic event (e.g., magnitude, etc.) control the likely shear strength reduction in the slopes, and chances of failure (Voight, 1978). Malamud et al. (2004) suggested that relatively small (c. 10^4 m^3) landslides can be triggered by earthquakes with threshold magnitudes of only M 4.3 ± 0.4. A landslide with a volume of 10^6 m^3 would require an earthquake of M 6, while one with a volume of 10^9 m^3 would require M 8. Keefer (1999) similarly estimated that gigantic rock avalanches (in the order of 10^9 m^3) would require earthquakes of $M > 8$. Finally, seismic events may reactivate existing landslides as well as trigger new failures.

9.2.1.3 Glacier Basins and Rock Avalanches

Evidence from various mountain ranges suggests massive rock slope failures are as frequent or more frequent in glaciated basins than in surrounding, ice-free valleys (McSaveney, 2002; Geertsema et al., 2006; Hewitt, 2009). It follows that glacier basin environments increase either preparatory and triggering factors, or both. Several elements may contribute:

1. glacier basins, at least outside high latitudes, are located in high, steep, tectonically and seismically active and densely fractured mountain ranges, recent from the geological perspective and with high erosion rates;
2. glacier erosion tends to greatly steepen rock slopes;
3. glacier shrinkage causes debuttressing of slopes; and
4. isostatic rebound resulting from regional deglaciation may generate stresses and fracture in bedrock.

In addition, triggering factors within, as well as outside glacier basins arise from higher seismicity due to tectonics, frequent and large freeze-thaw cycles, and permafrost in rockwalls or its degradation.

Remote sensing methods have made rock avalanches on glaciers visible as never before, and increase the chance of event detection before removal of the deposit. In contrast, reported frequencies of past supraglacial rock avalanches certainly underestimate them. Deposits are mostly in uninhabited, perhaps rarely visited areas where glacionival processes quickly remove the evidence. Once they are incorporated into moraines, or reworked by glaciofluvial processes, it may be difficult or impossible to detect them. Of particular relevance are the results of a study by Ekstrom and Stark (2013). They identified a unique seismic signature associated with landslides on glaciers. They found that one-third of the 29 landslides identified were previously unreported, including seven with a combined volume of c. 200 Mm^3 that descended onto Siachen Glacier in the Karakoram in September 2010. Otherwise, it seemed likely that these Siachen Glacier landslides would be misinterpreted as deposits of one or two extremely large slope failures or, perhaps, not recognized as landslides at all. Their technique is expected to facilitate identification of remote landslides.

Supraglacial rock avalanches that travel over moraines present an especially challenging interpretation problem (e.g., Deline and Kirkbride, 2009; Kirkbride and Winkler, 2012). Moreover, many recent supraglacial rock avalanches have been misinterpreted/identified as normal supraglacial cover, much as nonglacial examples have been interpreted as morainic complexes (Porter and Orombelli, 1981; Hewitt, 1999).

9.2.2 Supraglacial Motion

9.2.2.1 Flowing Processes

Rock avalanche movement has been described as "granular flow". Because of their high velocity, a collisional flow regime applies where energy is dissipated by contacts between individual grains. It has been suggested that frictional energy dissipation is reduced by dynamic, pore-pressure fluctuations due to grain rearrangement (Schneider et al., 2011b), but these are highly constrained, since clasts and original lithological units, although massively fractured and pulverized, maintain their relative positions in the mass. A slight dilation and intense local vibration or collisional chaos occurs. Rock fragmentation has been suggested to be a source of because it is the vibrational energy that reduces intergranular friction (Davies et al., 2010), because it is much more powerful than the purely vibrational energy due to grain rearrangement. The overall mass may spread, converge, split, or undergo large-scale shearing of superimposed debris sheets. However, in rock avalanche flow there is no turbulence and individual clasts cannot move through the mass. In other respects, the rock avalanche resembles a viscous fluid, and its deposits show well-defined flow features and preserve lithological relations in the original bedrock (Jibson et al., 2006). Distinctive properties of a glacier surface and its potential for erosion and ablation can modify rock avalanche behavior and also entrainment of ice and snow and their possible melting.

Depending on season, or descent over the glacier accumulation zone, the rock avalanche may encounter on-ice snowpack or firn. Particular rheological and movement features were identified with heavy snow covers on Alaskan glaciers in the post-1964 earthquake landslides (Post, 1967; Johnson and Ragle, 1968; McSaveney, 1978). Ice may be derived from failure zones, but is mostly entrained at the surface of the glacier, especially at icefalls (e.g., the Hochstetter Icefall during the 1991 Aoraki/Mount Cook rock avalanche; McSaveney, 2002). Mixed rock–ice deposits of rock avalanches have a wide range of ice contents (Table 9.1), from 15 percent at Sherman Glacier in 1964 (McSaveney, 1978) to 90 percent at Lyell Glacier (South Georgia) in 1975 (Gordon et al., 1978).

In 1997 at the Brenva Glacier (Mont Blanc massif, Italy), the collapse of ≥ 2 Mm^3 of granite rock mobilized a large amount of ice, firn, and snow along its 5.7-km-long path on the glacier. Although proportions of rock and ice/firn were roughly equal in the upper part, the distal part of the deposit (mean

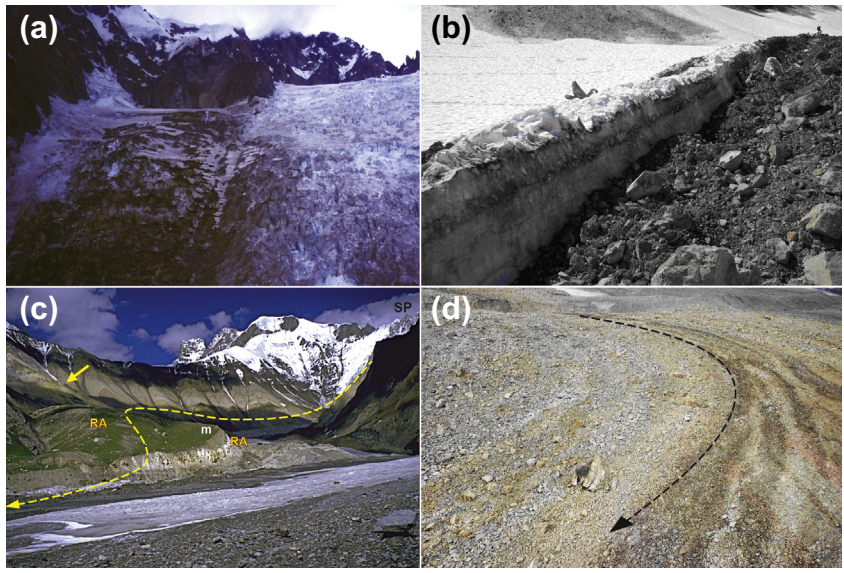

FIGURE 9.2 Flowing processes of rock avalanches onto the surface of glaciers. (a) Trough carved by the 1997 rock avalanche on the Brenva Glacier surface, Mont Blanc massif. The 2 Mm^3 scar is towering above the c. 15-m-deep trough *(Photo: P. Deline)*; (b) 2006 rock avalanche onto Jarvis Glacier, St Elias Mountains, British Columbia. The photograph, taken within a week after the event, shows melting of c. 2 m of firn as rock avalanche traveled over the glacier surface *(Photo: D. Capps.)*; (c) Gannish Chissh prehistoric rock avalanche, upper Barpu Glacier, Karakoram. It descended from Spantik Peak (SP), crossed the glacier to emplace crushed whitish crystalline limestone debris (RA) over moraines, and in >300 m run up of opposing slope (yellow arrow). Main lobe swung through 90° to travel 11 km downglacier to the left (dashed arrow). A surge-related lateral moraine (m) later covered the rock avalanche deposit *(Photo: K. Hewitt)*; (d) flow banding as the landslide changes direction, Black Rapids Glacier, Central Alaska Range; the arrow shows the flow path *(Photo: D. Shugar)*.

thickness >20 m) included 90 percent ice and firn. Some ice masses were as large as houses, even reported to be "as wide as the San Siro stadium in Milano, and as high as a 20-floor building". Total ice and firn volume was estimated at >4 Mm^3 (Deline, 2009)—the wide trough excavated down the glacier corresponded to c. 3 Mm^3 (Figure 9.2(a)). At that time (January), snow cover ranged from c. 150 cm at the glacier terminus to 300 cm at its head. Giani et al. (2001) modeled a mobilized snow volume of 5.4 Mm^3, of which 45 percent would have been incorporated in the accompanying snow powder avalanche. With c. 1 Mm^3 of packed snow included in the deposit, the total volume of ice/firn/snow mobilized by the rock avalanche was at least twice the collapsed rock volume.

When ice and snow are incorporated into a rock avalanche, thermal interactions occur: the frictionally heated debris may cause rapid melting of ice and snow and generate a water film. There is evidence of ice melting at the base and margins of some rock avalanches (Figure 9.2(b)), and of refrozen ice

within the Sherman Glacier rock avalanche deposit (Sosio et al., 2012). At Bualtar Glacier (Karakoram Himalaya), rapid ablation and, possibly, impact erosion by the 1986 rock avalanches changed initially rough, heavily crevassed surfaces to relatively smooth ones (Hewitt, 1988).

As in nonglaciated environments, rock avalanches on glaciers generally produce very large dust clouds resulting from the rock fragmentation, sometimes with air blast that reflects the high energies involved. Examples include Aoraki/Mount Cook in 1991, Punta Thurwieser (Ortles-Cevedale massif, Italy) in 2004, Monte Rosa (Italy) in 2007, Mount Steele (Yukon) in 2007, and John Hopkins Glacier (Alaska) in 2012. The cloud can contain snow or ice, and may act like a dry snow avalanche. The air blast triggered by the 1997 Brenva rock avalanche destroyed a >200-year-old forest along the opposite valley side, with a run-up exceeding 500 m. Skiers present described being plunged into semidarkness, and tree branches were pulled up and thrown about. The mixed icy-rocky dust pitted the windscreens of cars, and a 5-cm-thick layer of ice powder was deposited downvalley (Deline, 2001). Porter and Orombelli (1980) reported that birds were killed during the 1717 Triolet rock avalanche on the Mont Blanc massif, presumably by the air blast. At Jarvis Glacier (BC), the air blast from the 2006 rock avalanche killed a bird and spattered it with mud.

The highly mobile rock avalanche mass is sensitive to the geometry of the surface, tending to extend or compress over convex or concave surfaces, respectively. Where it encounters larger obstacles, the sheet may split into separate debris lobes. Remarkable heights of run-up on opposing slopes may occur. Debris from the prehistoric Gannissh Chissh (Spantik Peak, Karakoram Himalaya, 7,027 m a.s.l.) landslide was emplaced on the opposing valley wall more than 300 m above the glacier surface (Figure 9.2(c)).

Dufresne and Davies (2009) argue that certain surface features such as longitudinal flow bands are fundamental characteristics of granular flows on glaciers, and differ from the typical elongate ridges found on nonglacial landslides though both may be similar in terms of the ratio ridge spacing/flow depth. Flow bands can separate zones of different lithologies (e.g., Shreve, 1968) or grain size (e.g., Shugar and Clague, 2011), or simply represent shear between debris moving at different velocities. At Black Rapids Glacier, flow bands on the three 2002 rock avalanches indicate a variety of flow paths (Figure 9.2(d)). The westernmost rock avalanche spread relatively uniformly across the glacier, with little deflection downglacier. Flow bands on the central rock avalanche indicate that it turned abruptly downglacier as it encountered the lateral moraine on the distal side. Flow bands on the easternmost rock avalanche indicate that some of the debris traveled north across the glacier, before it turned to the east, downglacier. Much of the debris however, traveled directly to the northeast. At Sherman Glacier, 1964 flow bands indicate that the landslide spread as it traveled downglacier, but with no abrupt turns as at Black Rapids Glacier.

9.2.2.2 Higher Mobility of Rock Avalanches on Glaciers

Whereas horizontal travel distance for most landslides approximately equals vertical travel, for rock avalanches the ratio is much greater, up to 10:1 (Friedmann, 1997) and, on glaciers the ratio can be even higher. Various mechanisms have been proposed to explain this, irrespective of whether they travel over ice, and include water or air lubrication (Kent, 1966; Shreve, 1968), acoustic and mechanical fluidization (Hsü, 1975; Melosh, 1979; Davies, 1982; Collins and Melosh, 2003), and fragmentation spreading (Davies and McSaveney, 2002, 2009). These theories can be broadly categorized as those that reduce basal friction, and those that reduce internal friction (Davies et al., 1999; for a recent summary see Davies and McSaveney (2012)).

In their seminal study of 17 cases, Evans and Clague (1988) found interaction with glacier ice significantly enhances rock avalanche mobility, and by an average of 24 percent. Other studies confirm this, including by Dutto and Mortara (1991) comparing 15 rock avalanches onto glaciers with 16 in nonglacial environments (Figure 9.3).

Evans and Clague (1988, 1994) offer several hypotheses to explain the greater mobility of rock avalanches on glaciers versus those in nonglacial environments:

1. the debris travels on low-friction (i.e., ice and snow) surfaces; the apparent coefficient of friction (μ, corresponding to height-over-length, H/L, ratio) of the interface between rock debris and ice is low (Table 9.1), but a preexisting supraglacial debris cover can markedly increase friction;

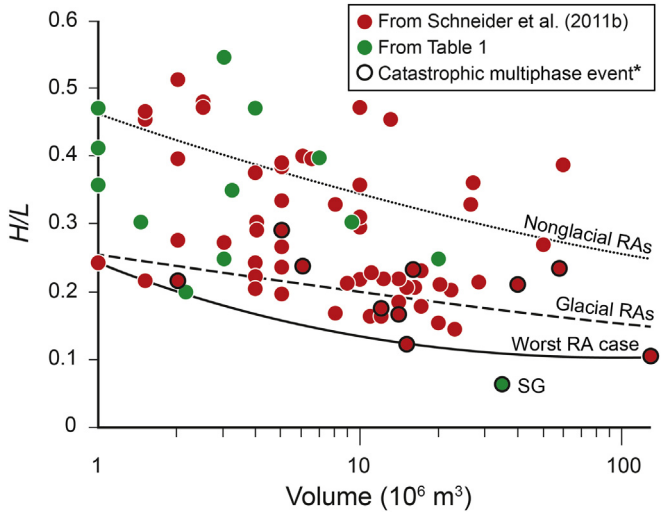

FIGURE 9.3 Mobility of rock avalanches (volume >1 Mm^3) on glaciers shown by the relationship between volume and ratio between vertical (H) and horizontal (L) travel distances; regression lines from Schneider et al. (2011b) and Evans and Clague (1988); SG, Steinsholtsjokull Glacier, Iceland; *, *sensu* Petrakov et al. (2008).

2. pore pressures are generated at the base of the debris by frictional melting. Sosio et al. (2012) model a reduction of the basal friction angle of >20 percent at Sherman Glacier through pore-pressure generation;
3. the debris is fluidized by melting ice and snow. A laboratory model of Schneider et al. (2011a) showed a reduction of the bulk friction angle is 13−50 percent for a mass of dry granular ice compared to a granular rock mass; and
4. the debris may be channelized or air-launched by moraines.

Evans and Clague (1999) later proposed that a significant volume of fine particles due to intense fragmentation of the source rock mass may enhance the mobility of a rock avalanche. It is not clear how this applies specifically to those descending onto glaciers. However, a significant difference between glacial and nonglacial rock avalanches relates to spreading. Most cases spread and thin, but Geertsema et al. (2006) suggested this is greater for travel over glaciers, a view supported by the fragmentation theory of Davies and McSaveney (1999). Compared to ice-free valleys in rugged terrain, glaciers tend to have more open surfaces allowing greater spread of the debris lobe and, consequently, producing much thinner debris sheets. Strom (2006) argued that, for unconfined rock avalanches, normalized debris deposit area is a better metric of mobility than linear travel distance, since friction acts over the entire basal surface. Recently, this has been demonstrated for a number of glacial and nonglacial rock avalanches (Shugar and Clague, 2011; Shugar et al., 2013a).

The high mobility of rock avalanches on glaciers causes enhanced velocities, generally >60−70 m/s (Sosio et al., 2012; Table 9.2).

9.2.3 Rock Avalanche Deposits and Sedimentary Properties

The character and fate of rock avalanche materials depend on original bedrock properties, the travel path, and where they come to rest (Table 9.3). On ice, subsequent modification occurs as part of supraglacial processes, including thermokarst, and final dispersal from, and deposition around the glacier. A critical distinction is between landslides that are wholly confined to a glacier surface, and those that travel over and beyond it. A suite of transitional situations may be involved. Where landslide material is encountered on ice, partial or intermediate rock avalanche properties may prevail. Deposits that are thick enough to prevent ablation may be passively transported. They can retain typical rock avalanche properties until finally released through thermokarst processes as the ice stagnates. However, dispersal to the margins increases moraine-like properties. Eventually some of the geomorphic and sedimentological diagnostics of rock avalanches may be lost.

If part or all the mass travels beyond the glacier terminus, deposits have the potential to survive in the landscape for millennia or longer. They may have some distinctive properties due to enhanced mobility and entrainment of snow

TABLE 9.2 Velocity of Rock Avalanches onto Glaciers

Rock Avalanche	U_{mean} (m/s)	U_{max} (m/s)	U at n km from Source (m/s)	References
1964 Sherman Glacier	26	67		Sosio et al. (2012)
1991 Aoraki/Mount Cook	55–58	100[1]		McSaveney (2002), Sosio et al. (2012)
1992 Mount Fletcher	80	120		McSaveney (2002)
2000 Tsar Mountain	22–45			Jiskoot (2011a)
2002 McGinnis Peak Glacier N			>54 at 4 km, >40 at 5 km	Jibson et al. (2006)
2002 Black Rapids Glacier E			>35 at 2 km	Jibson et al. (2006)
2002 Punta Thurwieser		63		Sosio et al. (2012)
2003 Iliamna Red Glacier		>80		Sosio et al. (2012)
2005 Mount Steller		100		Huggel et al. (2008)
2007 Mount Steele		65	>73 at 5 km	Lipovski et al. (2008)

[1]*Modeled* U_{max}.

and ice from the glacier. Materials emplaced along the ice margins may be incorporated into, or easily mistaken for, latero-terminal moraines. In general, materials emplaced beyond Neoglacial and, especially, Late-Glacial ice margins are disproportionately represented in the geological record. The incidence and full role of purely on-ice events can only be inferred.

For some time after initial emplacement, much or all of the material, even on the glacier, may retain distinctive rock avalanche properties in composition, facies, and assemblage morphology. Travel over the ice or entrainment of snow, ice, meltwater, and supraglacial debris may create some differences from nonglacial examples. In time, the materials undergo progressive modifications by supra- and englacial processes. On heavily crevassed surfaces, debris is irregularly emplaced and may create an envelope that is thicker over crevasses or depressions, and thinner over raised, convex, and smoother areas. McSaveney (1978) showed how such "wave crests and troughs" from the interaction of crevassed ice and rock avalanche trajectories, are amplified by subsequent differential ablation and ice movement (cf. Chillinji Glacier example in Section 9.3.2).

TABLE 9.3 Diagram of Four Emplacement Classes of Rock Avalanches Affecting Glaciers

	Origin		
Emplacement	On Slopes over Main Glacier	On Slopes over Tributary Glacier/s	On Slopes of Ice-Free Valleys
Over main glacier	Ia	Ib	–
Partially over main glacier or/and over its termini	Ib	Ib	III
In ice-free valleys with effect on main glacier	IIa	IIb	IV

Source: Modified after Hewitt (2009).

It is important to recognize the changing spatial dimensions and patterns of where, how quickly and in which parts of the on-ice deposit the modifications occur, including the role of past and contemporary changes in glacier mass balance. Large areas of pure, unmodified rock avalanche material may survive for decades, even as equally large volumes have been reworked and dispersed from other areas. What is found depends on the stage encountered. Eventually, on an active glacier, all the material will be transported to the margins and acquire the distinctive properties of ice-margin and proglacial deposition (Hewitt, 2009).

Where large quantities of moisture or wet sediment are absorbed, the dynamics and sediment properties of a rock avalanche may be transformed to those of debris avalanche, debris flow or more complex mass flows, whether deposited on or beyond the ice. Careful examination of these materials can, however, reveal sedimentary properties diagnostic of a rock avalanche origin, despite considerable alteration (Fauqué et al., 2009; Reznichenko et al., 2012).

9.2.3.1 Deposition onto Glacier Surface

The surface of rock avalanches is generally an openwork carapace of boulder-sized clasts (Figure 9.4(a)). This is, however, deceptive. Where the deposit is exposed below the carapace, it contains large quantities of finer-grained matrix materials (Figure 9.4(b)). The fragments consist of fractured (compressional) and shattered (impact) clasts, and pulverized fines, which form a matrix filling all the space between larger clasts (see below).

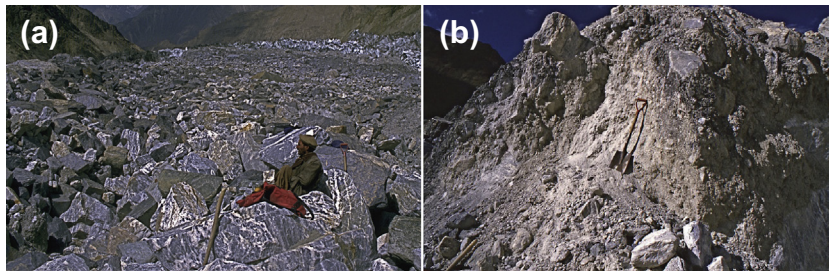

FIGURE 9.4 Deposit of the 1986 rock avalanches onto Bualtar Glacier, Karakoram. (a) Openwork carapace of boulder-sized clasts *(Photo: K. Hewitt)*; (b) cross section showing the large quantities of fine-grained matrix materials *(Photo: K. Hewitt)*.

Many researchers have qualitatively described geomorphic features of rock avalanche deposits, including raised rims, flow bands, and lithologic zonation. Little quantitative work, however, has been done to link debris sheet sedimentology to observed large-scale geormorphic features. Further, relatively little work has compared the sedimentary architecture of glacial and nonglacial rock avalanches, insofar as they relate to paleoclimatic reconstructions (e.g., Reznichenko et al., 2012; Shugar et al., 2013a). At Sherman Glacier, flow bands and subparallel grooves indicate the flow direction. At Black Rapids Glacier, the previously described longitudinal flow bands are alternating stripes of narrower fine debris and bands of coarse blocks on the rock avalanche surfaces. Flow bands at Black Rapids Glacier are characterized by differences in block (>1 m^2) size, with clusters of very large blocks (up to tens of meters long), especially in the distal reaches, separated by regions of much smaller blocks (Shugar and Clague, 2011). In comparison, the nonglacial 1903 Frank Slide (Canadian Rocky Mountains) exhibits no such flow bands, and the coarsest blocks are not concentrated in the distal reaches but in a band in the middle of the debris sheet (Shugar et al., 2013a).

9.2.3.1.1 Thickness of Rock Avalanche Deposits onto Glaciers

As a result of greater spreading across and down the glaciers, thicknesses of rock avalanche deposits are generally much less than those in nonglacial environments. In the Mont Blanc massif they are typically 1–5 m, an order of magnitude thinner than most off-ice cases. In the Chugach Mountains, Uhlmann et al. (2013) mapped 123 supraglacial landslide deposits >0.1 km^2, and found thicknesses ranging from less than a meter to several meters. Deposits of the seven larger rock avalanches triggered by the 2002 earthquake in Alaska, whose volumes are in the range 4–20 Mm^3, have an average thickness of 2–3 m (Jibson et al., 2006; Shugar and Clague, 2011), whereas the deposits of the small Vampire rock avalanches of 2003 and 2008 onto Mueller Glacier (0.12–0.15 Mm^3) in New Zealand have an estimated average

thickness of 0.5−1 m (Cox et al., 2008). At Jarvis Glacier (NW British Columbia), Evans and Clague (1999) observed average debris thickness of <0.5 m on a landslide triggered by the 1979 St Elias earthquake. At Bualtar Glacier, the debris thickness in 1987 was found to be quite variable, generally >2.5 m, in a few places over 10 m; exposures averaged between 3 and 5 m. After the 1991 Chillinji Glacier event, a few scattered vertical sections indicated similar thicknesses, averaging 3 m or more.

Thickness measurements are inherently difficult, and estimates are generally based on a few sampling pits or vertical sections revealed by erosion or ice collapse. For instance, McSaveney (2002) estimated that the 1991 Aoraki/Mount Cook deposit was 1.2 m average, whereas 250-m-long ground-penetrating radar (GPR) profiling from one edge of the deposit in 2009 demonstrated a thickness of 5−10 m (Reznichenko et al., 2011). GPR profiling on the West Fork Robertson Glacier (Alaska) deposit shows a variable thickness of 1.5−5 m (S. Herreid, written communication). Reduced ablation below the debris sheet causes the debris surface to become elevated above the adjacent ice, giving the appearance of greater thickness; while, conversely, erosion of the ice surface by the avalanche may cause it to incise into the glacier surface, giving the appearance of lower thickness.

9.2.3.1.2 Morphology, Sedimentology, and Macrofabric of Rock Avalanche Carapace

The large clasts of a surface rock avalanche carapace can acquire distinctive patterns or fabric in at least four ways:

1. remnant lithological bands: in these bands, boulder sizes and shapes stand out due to strength, structural units, or partings in different bedrock. The largest boulders will derive from the more massive or resistant rocks. It is of some interest to identify the largest clasts where they are salient features, and record the survival and shape of large units. Their size, shape, and emergence above the surface could serve as indicators of the transporting competence of these events, hitherto little investigated (Hewitt, 2002);
2. preferential alignment of largest clasts subparallel or at right angles to the direction of movement: this suggests that the largest boulders are preferentially oriented with movement vectors (e.g., Shugar and Clague, 2011). Smaller, blade, or rod-shaped blocks appear jostled by interaction with the larger blocks and lack preferential orientation;
3. "final moment" developments: imbrication, collisional fractures, and torque are observed in the surface boulders suggesting their movement stops irregularly if quite suddenly (Figure 9.5). There may be detachment of individual boulders or parts of the surface boulder sheet, which continue to move after the main body has stopped, especially if the main body matrix materials become saturated with meltwater. This was observed in the Bualtar Glacier rock avalanches in 1986 where some surface areas were

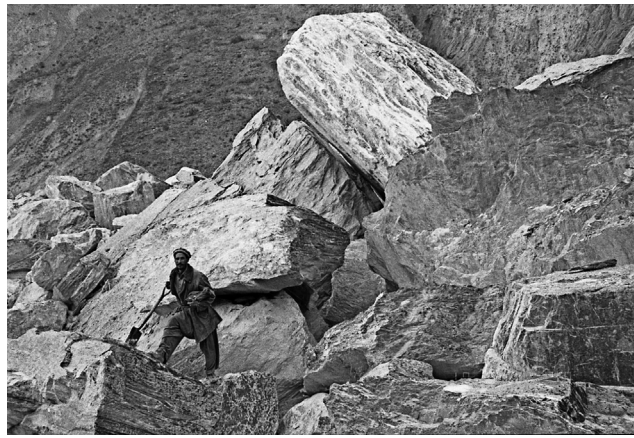

FIGURE 9.5 Imbrication in the surface boulders of Bualtar Glacier rock avalanche deposit of 1986, suggesting their movement stops irregularly if quite suddenly *(Photo: K. Hewitt)*.

left with few or no boulders, while concentrations of imbricated and jumbled boulders occurred downslide;

4. distal rim concentrations of largest boulders: this may be due to final moment detachment just mentioned. Possibly, blocks at the outer surface and lower, outer margins of the original failed rock slope escape the heaviest crushing forces in the initial descent, and maintain their outermost positions in the rock avalanche.

9.2.3.1.3 Matrix Particle-Size Distribution

The main body of a rock avalanche deposit generally contains a full spectrum of grain sizes from megaclasts (boulders exceeding 10 m diameter) to fine silts and clays. Grain-size distributions for matrix materials approximate a linear plot on a log-normal graph (Figure 9.6). Observations in the Karakoram indicate more than half the volume of rock avalanche deposits on glaciers usually lie in the range granule to fine-silt size grades. The Wentworth "sand-sized" fraction is the larger part of the matrix (Hewitt, 2002). Absence of clay-sized material may not only be due to little or no production. The moving mass may be sufficiently dilated for it to be dispersed and expelled with the compressed air to help create the great dust clouds observed in these events. Grain-size analyses of the 1991 Aoraki/Mount Cook rock avalanche sediment the day after the event showed 99.5 percent of the sampled fragments (by number) were <10 μm in diameter (McSaveney and Davies, 2007). A significant presence of fine particles was found in repeat studies nearly two decades later (Reznichenko et al., 2012). Grain-size analyses for the rock avalanche matrix on Black Rapids and Sherman Glaciers (Shugar and Clague, 2011) indicate predominant muddy sandy

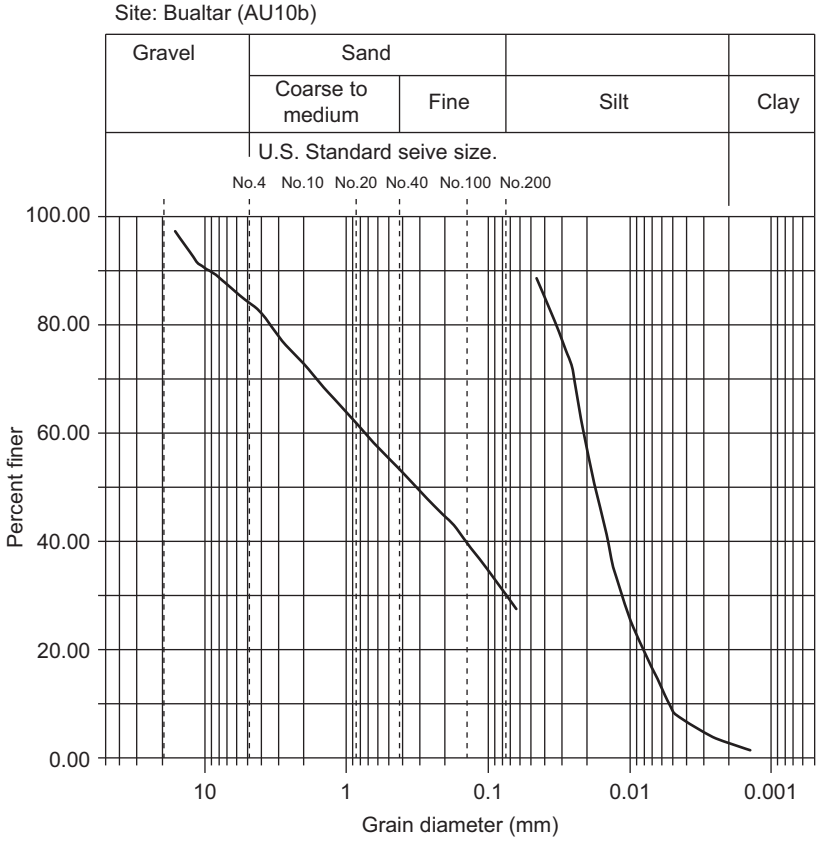

FIGURE 9.6 Grain-size curves for matrix material from Bualtar Glacier rock avalanche deposit of 1986. This sample is representative of a hundred samples, all very similar.

gravels, and generally less than 5 percent by mass of sediment <10 μm. The rock avalanche matrix samples from Black Rapids Glacier are significantly more poorly sorted than those from Sherman Glacier. One sample from a medial moraine on Black Rapids Glacier had c. 20 percent sediment <10 μm. This reported inconsistency of clay content in rock avalanche material may result from differences in the proportion of silt/clay size clasts to other size fractions varying between rock avalanches depending on the lithology of the parent rock, the volume of rock avalanche and its runout distance. Because in conventional grain-size measurements, it is rare to recognize grain sizes as small as <10 μm (Crosta et al., 2007), in many cases very fine particles adhere to the surfaces of coarser clasts or bond together into agglomerates, and thus may not be recognized as individual grains although formed during the event.

Reznichenko et al. (2012) developed a method to differentiate rock avalanche material from glacial sediment, using the presence of characteristic micron-scale features, missed by traditional grain-size analyses by sieve but seen under a scanning electron microscope (SEM). Silt- and clay-sized grains from rock avalanche sediment are typically agglomerates of numerous finer particles that survive the washing and dispersion of conventional grain-size procedures such as sieve analysis. The clasts appear angular and subangular, identical to parent material lithology, and clumped together by finer matrix of submicron size. This results from highly confined and nondispersed fragmentation of grains in the deposit during rock avalanche emplacement. The main point is that these agglomerates are entirely absent from glacial sediments: under SEM observations fine grains from glacial environments are solid and do not form clusters.

9.2.3.2 Postdepositional Modifications of Rock Avalanche Deposits on Glaciers

Rock avalanche deposits on large glaciers can survive supraglacially for decades and with little or no discernible change in the core areas. Where not otherwise disturbed, the whole deposit will gradually come to sit on a platform of ice 5–50 m thick, beneath whatever depths the landslide materials have. The apparent thickness of on-ice rock avalanche deposits observed after one or more ablation seasons, or in satellite images, must be treated with caution. The rate at which it can be raised is governed by absent or much lower ablation below the deposit compared to surrounding glacier surfaces (e.g., Reznichenko et al., 2010). However, thickening due to ablation protection generally seems to reach a limit at around 15–20 m suggesting that it is then compensated by increased ice flow at depth from beneath the raised areas (Hewitt, 2009). Differential ablation can also result in a hummocky topography and supraglacial thermokarst lakes with debris continuously reworked by relief inversion and backwasting.

9.2.3.2.1 Reworking of Rock Avalanche Debris

Rock avalanche deposits on a glacier are subject to a range of processes that can modify their composition, facies properties, and coherence. Ice movement, compression, divergence, and crevassing will disturb the debris sheet. Ice ablation can become the major modifier, especially at deposit margins and wherever ice becomes exposed or the debris thinned so that increased ablation causes local disturbance. Wind as well as meltwater winnows out the finer materials. Surface drainage can partially wash finer materials away, leading to coarsening and sorting of the residual deposits. However, these modifications are not necessarily rapid or complete. Transport on Tasman Glacier, and exposure to rain and snowmelt had not significantly winnowed the finer matrix noted in the 1991 Aoraki/Mount Cook deposit by Reznichenko et al. (2012; cf. 1.3.1.3).

Coarser fragments can be redistributed, comminuted, and crudely rounded by sliding and fallsorting, especially due to ablation-driven relief inversions. Freeze-thaw cycles, crushing between boulders, and splitting of large fractured boulders during supraglacial displacement, cause debris comminution, and lead to greater compactness. Material washed into on-ice ponds will become crudely sorted and stratified, but coarse blocks also tumble in to disturb and complicate grain-size distribution. On Black Rapids Glacier, Shugar and Clague (2011) noted dozens of large quartz diorite boulders that had been turned into sands and gravels in only 5 years of freeze-thaw activity.

Meanwhile, "normal" glacier processes continue and glacially derived debris becomes mixed with rock avalanche materials. They become mixed or interspersed with supraglacial moraines derived from vertical emergence of englacial debris septa (Eyles and Rogerson, 1978). Glacier tables can develop where rock avalanche boulders are or become dispersed away from the continuous deposit, but are more common in blocks fall-sorted along the margins of medial moraines, or from individual rockfalls.

9.2.3.2.2 Modification of the Pattern of Supraglacial Deposits

Eventually, rock avalanche deposits may be so modified as to resemble or be difficult to distinguish from other heavy debris covers. However, debris from other sources is rarely either as thick or monolithologic. Rock avalanche deposits also depart from the tendency of supraglacial moraines to show longitudinal and transverse gradients of debris thickness.

At Sherman Glacier for example, five decades of supraglacial transport have altered the morphology of the deposit. The flow bands created by shear during emplacement of the debris in 1964 now serve as passive indicators of differential ice velocity, and form arcuate lines, which are convex downglacier (Shugar and Clague, 2011). Fabric measurements in 2008 showed that the debris has been reoriented to reflect this post-depositional shear.

It can happen that several rock avalanche deposits are merged in a continuous supraglacial debris cover. The debris cover of the Miage Glacier (Mont Blanc massif) consists of several dozen morpholithological units resulting from rockfalls or rock avalanches. Units defined by lithology, fabric, and particle size, roundness and distribution, have areas in the range 5,000–300,000 m^2. Two types can be distinguished (Figure 9.7). Flow-parallel units (e.g., UD7, UD3) are stripes derived from rock avalanches and rockfalls onto the glacier accumulation area transported englacially, with some emerging at the glacier surface as debris septa. A straight stripe is associated with a short englacial transport path from emplacement close to the equilibrium line altitude (e.g., UD7). A curved stripe results from a longer englacial transport path (e.g., UD3a–c). The second type comprises irregular units (e.g., UD1) from rock avalanche and rockfall deposited in the

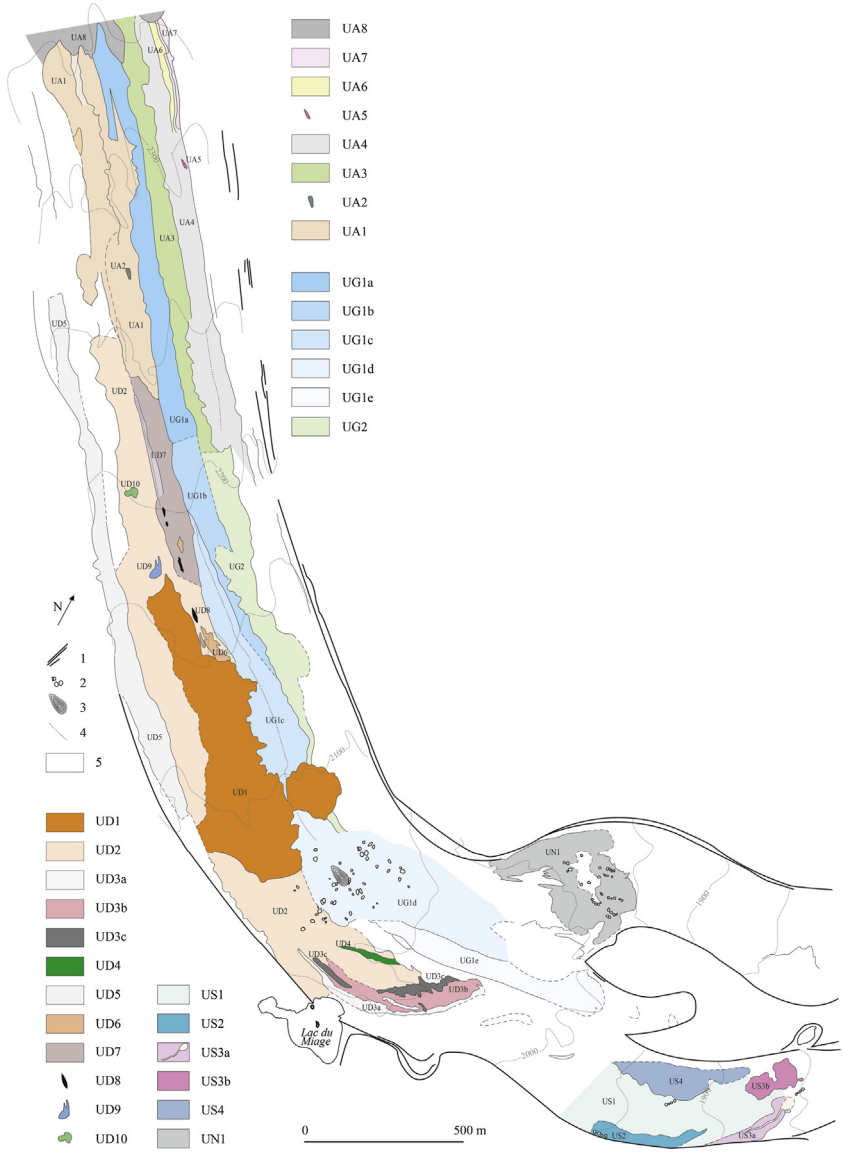

FIGURE 9.7 Morpholithological units of the debris cover of the Miage Glacier, Mont Blanc massif, in 1997, resulting from rockfalls and rock avalanches. 1, Moraine crest; 2, 3, mega-boulders; 4, debris septum; 5, area not mapped.

ablation zone. They have been transported entirely supraglacially, and have irregular shapes independent of the flow, but have sharp limits, homogeneity, and a hummocky topography due to numerous megablocks. At Miage, three irregular units correspond to dated rock avalanches that occurred during the

twentieth century (Figure 9.7). Large, flow-parallel units (e.g., UA1 or UD2) record earlier rock avalanches that affected the accumulation zone.

9.2.3.3 Deposition of Rock Avalanches outside the Glacier

Because of long runout, many rock avalanches may travel over and beyond smaller valley glaciers and sometimes even quite large ones. Dozens of examples are known in the Andes, the Caucasus, Pamir, Karakoram, Hindu Kush, and Greater Himalayan ranges, that spread far down river valleys below the ice; the longest so far identified has 28 km runout, at least half of which is beyond the glacier (Robinson et al., 2014). Those crossing glacier margins or valley junctions below, form some of the thickest deposits (>100 m) due to blocking and stalling of rock avalanche lobes against opposing slopes (Hewitt, 2006). Since these developments are more likely to pose serious hazards for human communities and infrastructure, the ability to reconstruct their role in the Holocene, at least, is a key to predicting future risk.

Deposits outside glaciers tend to have much less regular and thicker masses of debris, which may alternate with debris veneers. In humid mountains they can become obscured by vegetation after a few years. Ridges are common in mixed rock/ice deposits, but generally absent in the final debris deposit whose margins are usually raised and marked by a small talus. Finally, melting of ice and snow can result in a chaotic topography and chaotic sorting of debris. Clasts are mostly angular and subangular, but glacially rounded boulders entrained from moraines or from the proglacial margin are common. Smaller clasts are left piled and plastered over the larger boulders by ice melting. The silty-sand matrix may be reworked and flushed through the deposit.

Rock avalanche deposits outside a glacier may be mixed with those from other processes, and their morphology has led to confusing them especially with glacigenic or debris flow landforms and sediments. A critical example is in Val Ferret (Mont Blanc massif), whose morphology and composition led to prolonged discussion about the origin. There is an assemblage of morphologically distinct sectors with granite boulders covering a 2-km-long and 500 m-wide plain downstream of the moraine complex of the Triolet Glacier. In a topography dominated by hummocks and hollows are regions with chaotic blocks up to 1,000 m^3 in size, and with an openwork structure. There are 1–5 m-high concentric ridges consisting of matrix-supported diamicton, with megablocks on the crest. The deposits were reworked or partly buried by alluvial fill, late-LIA moraines, and polygenic debris cones supplied by runoff, debris flows, snow avalanches, and rockfall (Deline and Kirkbride, 2009).

Although de Saussure (1786) initially described a rock avalanche deposit on Triolet Glacier, many authors have since interpreted the entire deposit, or parts of it, variously as sets of moraines (Agassiz, 1845; Sacco, 1918; Zienert, 1965; Mayr, 1969; Aeschlimann, 1983), or glacial outburst flood deposits (Virgilio, 1883). Porter and Orombelli (1980) and Orombelli and Porter (1988)

were the first to ascribe the entire Val Ferret deposit to the CE 1717 rock avalanche. This was discussed by Deline and Kirkbride (2009) but confirmed by Akçar et al. (2012, 2014) using geomorphic mapping and radiocarbon dating, and cosmogenic ^{10}Be dating, respectively.

Glaciers may also readvance over rock avalanche deposits that act as barriers early in the readvance. If not fully reworked and dispersed, a complex, "trans-glacial" geomorphology and sedimentology result (Iturrizaga, 2006; Hewitt, 2013b). An example is the White Horse complex at the terminus of Mueller Glacier, Southern Alps (NZ). The deposit has a large debris nucleus most probably of rock avalanche origin that has locally affected glacier readvances during the last couple of thousand years. As a result, the glacier has partly overridden it and been deflected around its moraines. Similarly, Cook et al. (2013) describe an advance of Fee Glacier, Switzerland, over a rock avalanche deposit. This small glacier, with limited ice flow and erosion potential, was not able to rework the rock avalanche deposit, which resulted in partial preservation of the deposit's characteristic features, including brecciation, a coarse carapace, angular clasts, and hummocky topography. These deposits in the proglacial valley affect glacier readvance, slow its progress and may help form another heterogeneous, or trans-glacial deposit.

9.3 CONSEQUENCES

9.3.1 Rock Avalanche Contribution to Supraglacial Debris Covers

Rock avalanches are just one, instantaneously large but relatively infrequent, source of material to mountain glacier surfaces. Other more common and widespread processes include debris delivered in snow and ice avalanches; rockfall and debris flows; and erosion along proximal sides of lateral moraines by gullying, wind action, boulder fall, and slide. The latter tend to contribute more where the glacier surface is lowered. Debris incorporated in accumulation zones emerges at the ice surface downglacier from sub- and englacial transport paths either along shear zones or from ablation and in vertical debris septa, or by exposure of englacial channels. The proportion delivered by each source depends upon terrain steepness, geologic, geomorphic, glaciological, and climatic conditions.

Diagnostics of morphology and sedimentology of supraglacial rock avalanche deposits developed in recent years help make these sources more readily discriminated. The debris sheet is usually some meters thick, lies on a raised platform of ice up to tens of meters thick, and is composed of coarse material capping a matrix of finely pulverized material. It has a relatively high bulk density compared with other supraglacial debris. Samples reveal the monolithological and unsorted angular clasts in all size

fractions (Dunning, 2004; McSaveney and Davies, 2007; Hewitt et al., 2008; Reznichenko et al., 2012). Non-rock-avalanche sourced, supraglacial sediment has not undergone such intense fracturing and pulverizing so is generally coarser (Reznichenko et al., 2012), but also lacks the very large boulders characteristically associated with rock avalanches.

The sheer volume and physical properties of rock avalanche sediments help to discriminate them from more commonly observed supraglacial debris and materials from other subaerial sources. A rock avalanche immediately contributes an enormous mass of sediment (up to several km^3). Although relatively thin compared to rock avalanche deposits off-ice, the on-ice component is usually much thicker than even the heaviest, "normal" supraglacial debris. It can remain an area of conspicuously thicker debris during transport toward the glacial terminus. By comparison the more or less continuous exhumation of "normal" meltout debris annually or even over some decades adds very little and the cover may change little (Hewitt, 2009). Snow avalanche debris, boulder falls and most rockfalls are several orders of magnitude smaller than rock avalanches, and their individual clasts or blocks move largely in isolation from each other (Fort et al., 2009). In high mountain basins, the quasi-constant supply of material that results in "debris-covered glaciers" rarely exceeds an average thickness greater than 0.5−1 m, increasing gradually but systematically toward the glacier terminus (Nakawo et al., 2000). The debris contribution to the supraglacial cover originating from glacial erosion is estimated to be less than 1 percent of the volume of the ice melted in the ablation zone.

The 1991 Aoraki/Mount Cook rock avalanche deposit was on the order of 5−10 m thick (Reznichenko et al., 2011). Sediment delivery onto the Tasman Glacier from this one event exceeded 100 years of "normal" glacial sediment budget from all other processes.

The rock avalanche deposited on the Lyell Glacier, South Georgia, in 1975 is estimated to contribute at least 93 years' worth of sediment from subaerial erosion (Gordon et al., 1978). At Bualtar Glacier in the Karakoram, transport of the 1986 rock avalanche debris to the terminus in 30 years, including two surges, was equivalent to 500 years of supraglacial transport based on the prelandslide supraglacial cover and movement (Hewitt, 2009). At Miage Glacier, over 75 percent of debris derives from rockfall and rock avalanche. The lower Brenva Glacier was more than 90 percent covered by the 1997 rock avalanche (Deline, 2009).

Even with a low frequency, and certainly with one large event per century as indicated for many of the glacier basins identified here, rock avalanche inputs can still hugely increase the total sediment delivery. Also, for mountain glaciers, the substantial amounts of fines delivered almost instantaneously challenge the view that fine glacial sediment comes only from basal crushing and grinding by ice (Boulton, 1978; Davies, 2013).

9.3.2 Glacier Dynamics in Relation to Rock Avalanche Deposits

On-ice debris sheets can reduce or prevent ablation for years or decades and bring glacier thickening and advances out-of-phase with climatic conditions and surrounding glaciers (Shulmeister et al., 2009; Reznichenko et al., 2010, 2012). Unless recognized, these compromise glacial chronologies presumed to record only climatic fluctuations, especially in high mountains where massive rock slope failures are relatively frequent (Deline, 2009; Kirkbride and Winkler, 2012; Hewitt, 2013a).

9.3.2.1 Glacier Advance and Velocity Change due to Rock Avalanches

During times of climate warming, termini of debris-covered glaciers retreat less than those of clean glaciers. In the Mont Blanc massif, Mer de Glace (mainly clean) and Miage Glacier (debris-covered) have retreated 2400 and 300 m, respectively, since the 1820s LIA maximum (Figure 9.8). Conversely, advances of debris-covered glaciers last longer or reach farther downvalley. Triolet Glacier experienced a long-term advance after the CE 1717 rock avalanche: several decades later, de Saussure (1786) reported that it had been advancing for at least 8 years whereas the neighboring Pré-de-Bard Glacier was retreating. Triolet supraglacial debris cover, ascribed by Saussure to the rock avalanche, prevented ablation over much of the glacier, causing it to advance beyond the climatically controlled LIA limit. Although both glaciers currently have a similar area (c. 3 km^2) at a comparable elevation, the Triolet—which has not been debris-covered for about one century—has its current terminus standing c. 500 m higher than that of Pré-de-Bard although their LIA termini were at a similar elevation. Since then, the former retreated by 3 km but the latter by only 1.5 km (Figure 9.9: inset).

In 1913, Brenva Glacier began advancing, and by 1919–1920, was creeping forward at a rate of 20–25 m/a. In 1920, a rock avalanche of >2.4 Mm^3 of rock and >7.5 Mm^3 of ice covered the whole lower glacier and part of the upper glacier (Deline, 2009). Glacier advance increased to 43 m/a in 1920–1924, peaking at 55 m/a between April 1922 and June 1923 (Valbusa, 1924). The glacier advanced a total of 490 m between 1920 and 1941, whereas neighboring glaciers in the Mont Blanc massif retreated from the mid-1920s (Figure 9.8). Brenva Glacier has been retreating since 1989. From an average of 24 m/a between 1993 and 1996, the retreat rate decreased after the 1997 rock avalanche to 12 m/a in 1999–2001, with a possible readvance in 2008–2009 (Imhof, 2010). Thus, twentieth century rock avalanche deposits sped up the 1920s Brenva Glacier advance, and slowed retreat since the 1990s.

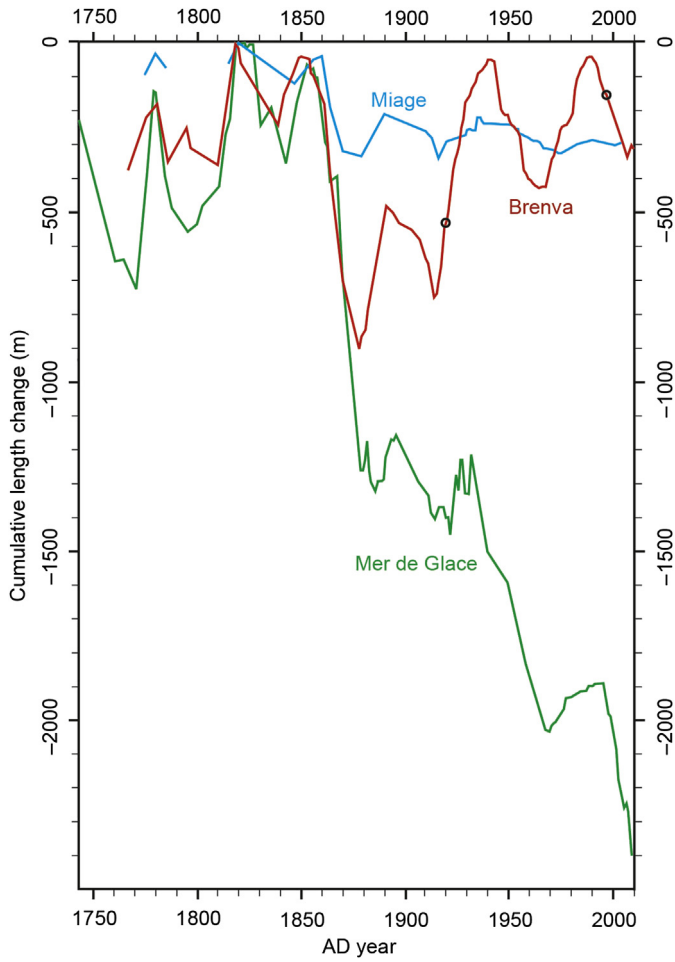

FIGURE 9.8 Cumulative length variations of the Mer de Glace (clean-type glacier), and Miage and Brenva Glaciers (debris-covered glaciers) since the end of the eighteenth century. Black circles: Brenva rock avalanches in 1920 and 1997. *After Imhof (2010), Nussbaumer et al. (2007), Vincent et al. (2012).*

Within 15 years of the 1964 rock avalanche at Sherman Glacier, Alaska, the debris sheet's distal edge had moved downglacier to the terminus. The landslide also caused the glacier to begin advancing (Figure 9.10). Between 1964 and 2011, the glacier advanced c. 0.5 km (Shugar et al., 2013b). At Black Rapids Glacier, Shugar et al. (2012) used satellite radar and ground surveying to measure surface ice velocity in the vicinity of the three 2002 rock avalanche deposits. It increased 44 percent within 2 years of the landslides, and then decreased to about the pre-2002 velocity. Interestingly, the velocity gradient, expressed as the difference between the velocity at the upstream and

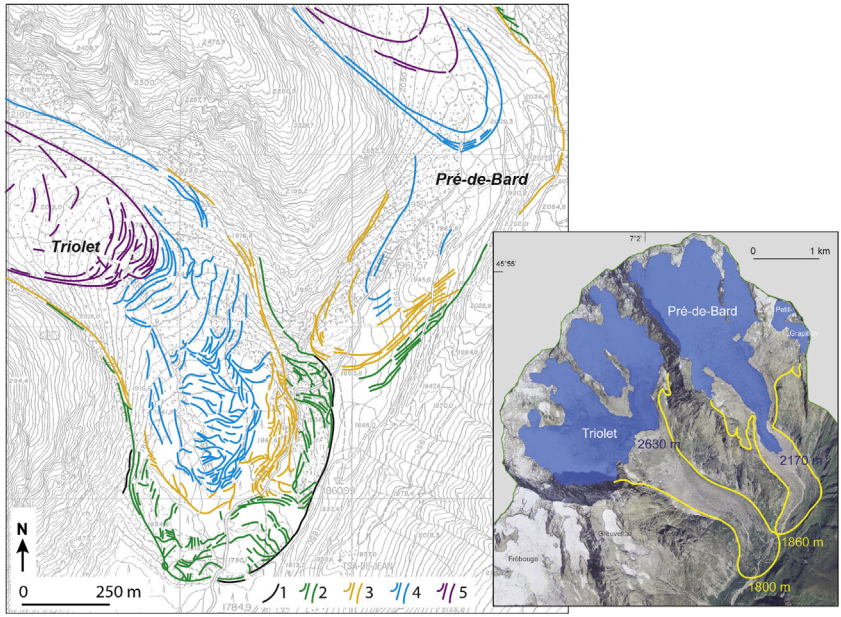

FIGURE 9.9 Map of the recent moraine complexes of Triolet and Pré-de-Bard Glaciers, Mont Blanc massif. Moraine ages: 1, possibly ante-CE 1717; 2, Triolet: post-CE 1717; Pré-de-Bard: seventeenth to eighteenth century; 3, CE 1820−1850; 4, CE 1860−1920; 5, 1920s. Inset: 2005 (blue area) and Little Ice Age (yellow line) extents of Triolet and Pré-de-Bard, with corresponding terminus elevation (Deline and Kirkbride, 2009 modified).

downstream ends of the debris sheet, dropped nearly to zero: in other words, in the vicinity of the landslide debris, the glacier was moving nearly uniformly. To confirm whether this significant change was triggered by the landslide, Shugar et al. (2012) used a Full Stokes 2D finite element model to elucidate the ice dynamics response to the debris sheet. The model reproduced the observed velocity gradient reduction, suggesting that landslide-induced mass balance changes were the cause. Changes in ice surface slope, resulting from reduced ablation under the debris and greater emergence velocities at the downglacier than at the upglacier end, pivoted the glacier surface toward the horizontal, resulting in a uniform longitudinal velocity profile. Black Rapids Glacier thickness is on the order of 600 m (Heinrichs et al., 1995), with the landslide debris just 2−3 m thick.

Chillinji Glacier in the Karakoram has had a somewhat similar response to Black Rapids since the 1991 rock avalanche (see Section 9.3.2). However, within a few months of the rock avalanche emplacements on their surfaces, Lokpar−Aling and Bualtar Glaciers went into surge-type accelerations 10 times faster than prelandslide velocities and massively disturbed the glacier tongues and ice-margin conditions (Hewitt, 2009).

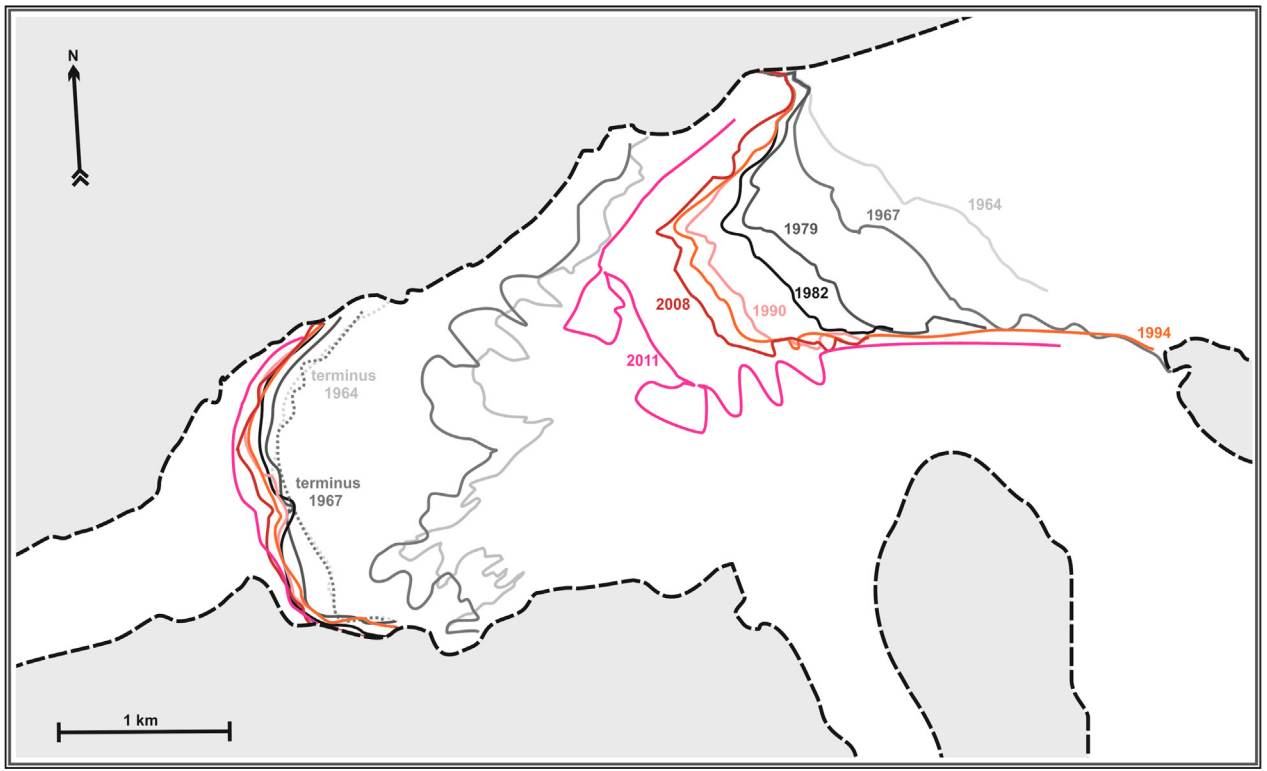

FIGURE 9.10 Changes of the rock avalanche deposit transportation since its 1964 supraglacial deposition onto the Sherman Glacier, Alaska, obtained from satellite and aerial images. During first 15 years the deposit distal edge reached glacier terminus and since caused glacier to start its readvance, while the upper edge moved >2 km downvalley, modified by the differential surface ice flow.

FIGURE 9.11 A 2-m-thick sheet of the 2002 rock avalanche debris overlie a 15-m-high ice platform in the ablation zone of Black Rapids Glacier, Alaska *(Photo: J.J. Clague)*.

9.3.2.2 Reduced Ablation due to Rock Avalanche Deposits

Debris cover on a glacier is an effective insulator that can substantially influence the ablation component of mass balance. Debris thickness and thermal conductivity together determine the thermal gradient, and impact on ablation rates. Debris thickness has the largest effect, hence the exceptional potential for rock avalanches to influence this factor. A 20 cm debris cover may reduce daily ablation by six times compared to clean ice and a meter or two shut it down altogether (Nakawo and Rana, 1999; Reznichenko et al., 2010). Debris-draped ice platforms may increase in thickness by several meters per year and reach heights of many tens of meters (Figure 9.11). Undisturbed rock avalanche sheets are near-perfect insulators under cyclic thermal inputs (Reznichenko et al., 2010). Thermal conductivity is important in normal debris covers and degraded landslide covers; in addition to the effect of thickness, thermal conductivity can vary with the mineralogy, porosity, and moisture content of the debris, its albedo, and water and air circulation (Mihalcea et al., 2007).

9.3.2.3 Effect of Load Increase and Subglacial Drainage Change

It seems unlikely that simple loading will significantly affect glacier dynamics, as the thickness of rock avalanche deposits on glaciers is limited by the increased mobility imparted by travel over ice—deposits >5-m-thick on average are generally associated with very rough, resistant substrates or stalling against an opposite slope. In the Karakoram for example, the thickness of ice protected from ablation in 4–6 weeks of summer by rock avalanche debris exceeds the landslide mass and thickness (Hewitt, 2009b). No known rock avalanche has been as thick or as great in mass as the brittle upper zone of ice that loads the underlying part where creep deformation occurs, so it is a

small addition to the loading of the latter. On relatively thin glaciers, shock loading from rock avalanches may be significant—perhaps causing catastrophic collapse and rock–snow–ice avalanches (cf. Chapter 7 in this volume, and thereafter)—but, to date, no studies have examined this. The frictionally heated rock mass may generate a sudden increase of meltwater in the cold season, at least, but such an effect also awaits research.

Some have thought that the 2002 Kolka–Karmadon event, which claimed 125 lives in the Genaldon valley in North Ossetia, Caucasus, was a catastrophic effect of mass load increase. On September 20th the glacier detached catastrophically from its bed, and over 130 Mm^3 of ice and rock swept downvalley 19 km, then transforming into a mudflow (or debris flow) that traveled a further 15 km (Huggel et al., 2005; Evans et al., 2009b; Sosio, in this volume). The event is not unique in Kolka Glacier history. In July 1902, the glacier underwent a two-stage detachment, the resulting mass flow traveling 11 km and killing 36 people. Three hypotheses have been proposed to explain these events:

1. The glacier is surge-type. Kotlyakov et al. (2004a) proposed a 2002 surge may have resulted from high water pressures within and beneath the glacier. However, when it surged in 1969–1970, the glacier remained connected to its bed. Further, there was no indication of a surge during the summer of 2002 (Huggel et al., 2005).
2. A detachment triggered by the impact of a collapsing mass of 20 Mm^3 of ice and rock onto the glacier (Huggel et al., 2005). Kolka Glacier was relatively thin in 2002—ranging from 85 to 175 m. If a large rock avalanche, on the order of 10 Mm^3 as reported by Huggel et al. (2005) descended onto the glacier, conceivably large glaciological changes would occur. However, Evans et al. (2009b) could find no firm evidence for such a rock avalanche.
3. Load increase by ice and rock deposits due to repeated collapses (15 Mm^3). Sporadic but significant snow avalanches, rock and icefalls went onto the surface of Kolka Glacier through the preceding summer months. It has been suggested this was enough to disrupt drainage within the glacier, and generate high subglacial water pressures. Enhanced geothermal activity was another possibility. Decreased effective stress and frictional resistance may have detached the glacier at the bed (Evans et al., 2009b).

Among the hypotheses that have been proposed to explain the almost complete erosion/entrainment of Kolka Glacier, some favor a model where factors affecting basal and englacial water seem critical. The highest levels of subglacier water pressure and destabilized mass may have involved a combination of pre-event conditions, such as higher rate of precipitation and summer ablation 1.5 to 2 times higher than average (Kotlyakov et al., 2004b), and the presence of hot geothermal springs close to the glacier (Muravyev, 2004). Documented seismic and volcanic gas activity prior to the event, and

eyewitness reports of explosive activity under the Kolka Glacier during the event, support the view that geothermal activity contributed. Loading by ice-rock debris may have been a factor further generating excess water pressure within and beneath the glacier (Fountain et al., 2005), perhaps causing a dramatic reduction of the frictional resistance that triggered the catastrophic failure (Evans et al., 2009b).

Bualtar was a known surge-type glacier before the 1986 landslides occurred but the landslide debris mass was less than annual ablation losses making it unlikely that loading was a factor. Massive injection of meltwater caused by the frictionally warmed debris is a possible factor—especially if the glacier was close to the surge threshold (Gardner and Hewitt, 1990). In all, these relations and mechanisms are poorly understood.

9.3.3 Moraine Complexes

High mountain glaciers, especially debris-covered ones and those that surge, often construct atypical moraine complexes, i.e., complexes with a disorderly pattern and/or at least partly disconnected from the regional climatic signal (Benn et al., 2003; Larsen et al., 2005; Hewitt, 2013b). When debris is supplied by rock avalanches even more complex developments occur, at odds with commonly inferred climate-driven glaciation and sedimentology.

9.3.3.1 Atypical Moraine Complexes and Implications for Paleo-Glacial Sequences/Reconstruction

Some 60 rock avalanches descended onto glaciers in the 1964 Alaskan earthquake. Dozens of rock avalanches are known to have affected the glaciers in the Karakoram Himalaya, possibly several thousand events in the Holocene alone (Hewitt et al., 2011b). At a more local scale, more than a dozen Holocene rock avalanches have occurred onto the Brenva Glacier below the Mont Blanc summit. These challenge the assumption that any major thickening, advance or moraine positions generally reflects regional climate cooling events, and related mass balance changes (Kirkbride and Winkler, 2012). They suggest the rock avalanches are recurrent, geologically "normal" processes in these, and perhaps most, high mountains. Major questions arise for glacial chronologies that fail to recognize and differentiate landslide-related episodes and deposits. This is compounded where surge-type instabilities are common, as in the Southern Andean, Alaska–Yukon, Caucasus, Pamirs, and Karakoram Glaciers. Moraine evidence for the major glaciations and longer-term climate-related glacial stages should be reliable but not, perhaps, their details.

Such problems have been identified with the Late-glacial Waiho Loop moraine in New Zealand, and debate about whether glaciers in the Southern Alps advanced during the last glacial–interglacial transition about 12–13 kyr BP, or "Younger Dryas" (e.g., Denton and Hendy, 1994; Barrows et al., 2008;

Applegate et al., 2008). A recently reinterpreted Antarctic Cold Reversal about 13 kyr BP is also involved (Putnam et al., 2010). A detailed sedimentological and morphological examination of the moraine shows that the Waiho Loop records the impact of a large, early Holocene rock avalanche on glacial mass balance and dynamics (Tovar et al., 2008; Shulmeister et al., 2009; Reznichenko et al., 2012). Given the typical arcuate terminal moraine shape of the Waiho Loop, Shulmeister et al. (2009) suggest it was emplaced by a Franz Josef Glacier advance, in turn due to a supraglacial rock avalanche. Using a one-dimensional numerical ice-flow model, Vacco et al. (2010) confirmed that this is plausible. Deposition of an extensive blanket of ablation moraine to its rear was subsequently confirmed at the base of the moraine and under the Tatare River gravels (Shulmeister et al., 2010). Geological and geochronological evidence (Wardle, 1978; Denton and Hendy, 1994; Tovar et al., 2008) suggests the glacier terminus was located between Canavan's Knob and the Waiho Loop when the rock avalanche occurred, requiring an advance of 3 km or less. The reduced ablation rate caused by the $\geq$100 Mm^3 of estimated debris is considered sufficient to affect mass balance enough to form the Waiho moraine. More recent work (Alexander et al., 2014) suggests that in order to form the uniquely high and steep moraine, the glacier terminus must have been at the Loop position when the rock avalanche occurred; thus no advance would have been involved, but instead a prolonged terminus still stand allowed the advection of a large quantity of supraglacial debris to form a single arcuate location.

Most of the Triolet moraine complex comprises a discontinuous and disorderly pattern of short ridges, unlike the few subconcentric moraines of the neighboring Pré-de-Bard foreland (Figure 9.9). The former relate to a heavy supraglacial debris cover on the Triolet from the 1717 rock avalanche. The post-1717 advance thus triggered was followed by a slow retreat over two centuries. A chaotic disintegration of the stagnating, debris-laden terminus was interspersed by minor glacial advances until the 1920s (Figure 9.9). Finally, debris-covered dead ice persisted upstream of the 1920s moraines from 1935 to the 1980s after the separation of the valley tongue from the active glacier (Deline and Kirkbride, 2009).

In these and other cases, the misinterpretation of moraine patterns resulting from mass balance alteration by rock avalanches as due to climatic signals raises doubts about glaciological, and hence, palaeoclimate reconstructions, at least those based on valley glaciers. Many rock avalanche deposits have been misidentified as glacial due to the morphological similarity and proximal position. Some sediment characteristics of rock avalanche deposits (fragmented mass of angular to very angular clasts and usually monolithology) are readily confused with supraglacial moraine in lithologically unvarying catchments. Diagnostic techniques are required to reliably distinguish rock avalanche affected moraines, such as that developed by Reznichenko et al. (2012) using the SEM (cf. 1.3.1.3).

9.3.4 Postlandslide Developments and Hazards

Rock avalanches onto glaciers can trigger or eventually lead to other dangerous consequences. These include glacier advances (sometimes sudden) and large dambreak and outburst floods from lateral-margin, englacial, or proglacial lakes. In a few cases they may trigger or accelerate the incidence of glacier surges. One surge immediately followed a rock avalanche onto the Lokpar Glacier tributary (Karakoram) in 1990. It disturbed and released an ice-margin lake that had existed for a century or more; the glacial lake outburst floods (GLOF) destroyed a summer village, forest and pasturelands down the valley (Hewitt, 2009). The main Aling glacier advanced up to 3 km in a decade. Many old rock avalanche deposits in the NW Himalaya and Karakoram have also become sources of repeated debris flows in rainstorms and heavy snowmelt, and include places where the highways are most commonly blocked by them.

The most extreme chain of high magnitude processes has been called a "catastrophic glacier multiphase feature" by Petrakov et al. (2008). It can involve a large ice-rock or rock avalanche traveling onto a glacier that transforms into a catastrophic mass flow (debris avalanche or flow) whose momentum and rheology allow it to continue far beyond the source slope and glacier margins. It may also generate a rapid glacier response due to insulating supraglacial debris deposit and glacier drainage changes. The best-known examples with exceptional runout and megaslide dimensions have continued far downriver systems into inhabited areas where they can cause great devastation. They exhibit greater velocities and longer runout than pure rock avalanches, commonly with massive entrainment of materials and progressive fluidization along the path. Some of the best-known cases originated in combined massive rock slope failures and large ice collapses (e.g., Nevados Huascaran, 1971) or impact and travel over glaciers typically destabilizing them (e.g., Kolka-Karmadon, 2002), and/or incorporation of vast quantities of snow, ice, and moraine (Horcones, below).

In the upper Indus basin more than 15 prehistoric supraglacial rock avalanches have been identified that traveled far into fluvial valleys downstream. They include particularly deceptive ones that emplaced tens of meters of erosion-resistant hummocky, mixed debris in the lower part, damming valleys in most cases (Hewitt, 2006). These landslide dams can affect a much greater area than the landslide itself through inundation, effects on fluvial sedimentation, or through a subsequent dambreak flood. The outburst floods may be much larger, and duration of geomorphic control can be much longer than in ice or moraine-ice dams caused by glaciers.

9.4 CASE STUDIES

The systematic overview of the topic given above needs, finally, to be filled out by actual events, and a sense of the details and complexities that enter into them. We choose three here; two recent ones from the Southern Alps of

New Zealand and the Karakoram Himalaya, and a prehistoric case in the Argentinian Andes, reconstructed entirely from deposits and the landform legacy.

9.4.1 Recent Rock Avalanches onto Glaciers in Aoraki/Mount Cook Area, New Zealand

Numerous small and several large rock avalanches have recently descended onto glaciers in Aoraki/Mount Cook area, Southern Alps, New Zealand. Their frequency has varied from one in every ten to hundred years (Cox et al., 2008; Allen et al., 2011). In the past 25 years the largest originated from the High Peak of Mount Cook (3,754 m a.s.l.) on December 14, 1991. It traveled across the Grand Plateau, down the Hochstetter icefall and spread over the Tasman Glacier. The $11.8 \pm 2.4\ Mm^3$ mass of rock (96 percent) and ice/snow (4 percent) fell 2,720 m and traveled about 7.5 km in 2 min; an average speed of 60 m/s. During the travel over the Grand Plateau and the Hochstetter icefall the deposit incorporated a large amount of ice, increasing the ice content more than 10-fold (50 percent by mass) (McSaveney, 2002). The landslide generated a magnitude M 3.9 earthquake (McSaveney, 2002). By 2011 the Hochstetter ice stream had deformed and separated the deposit into two main parts. An almost stagnant northern-eastern part traveled supraglacially about 500 m. The south part was rapidly modified and carried downvalley by the Hochstetter ice stream (Figure 9.12(a) and (b)). The deposit, up to 10 m thick, almost eliminated underlying ice ablation and caused the ice to thicken more than 30 m (Reznichenko et al., 2011). The debris volume was roughly equivalent to 180 years of average prelandslide debris flux through the icefall (Kirkbride and Sugden, 1992). However, the rock avalanche deposit covered less than 4 percent of the glacier ablation zone, too little to substantially influence flow velocities or mass balance (Reznichenko et al., 2011). The Tasman Glacier downvalley of the deposit remains in a state of rapid downwasting and retreat through proglacial lake calving and thermokarst development (Hochstein et al., 1995).

In the last 150 years at least four other massive rock slope failures have descended from the Aoraki/Mount Cook range. In 1873, a rock avalanche from Aoraki/Mount Cook (Barff, 1873), similar to or larger than the 1991 event, descended onto the Hooker Glacier, on the west side of the range. Smaller events occurred at Mount Vancouver (c. 3,300 m a.s.l.) in 1974 and Anzac Peak (c. 2,530 m a.s.l.) in 1991 (McSaveney, 2002). In 2013 c. $1.5\ Mm^3$ rock avalanche fell 500 m from Mount Dixon (c. 3,000 m a.s.l.) and covered about $1\ km^2$ of the Grand Plateau (Figure 9.12(a) and (c)). Satellite images and eyewitness video show that the rockslide partially eroded the glacier.

In November 2004 a rock avalanche from Mount Beatrice (2,528 m a.s.l.) buried a debris-free part of Hooker Glacier's ablation zone. It fell 440 m from an elevation between 1,620 and 1,700 m. Small rockfalls had been observed previously in the same area (Cox et al., 2008). GPR surveying in 2009 revealed

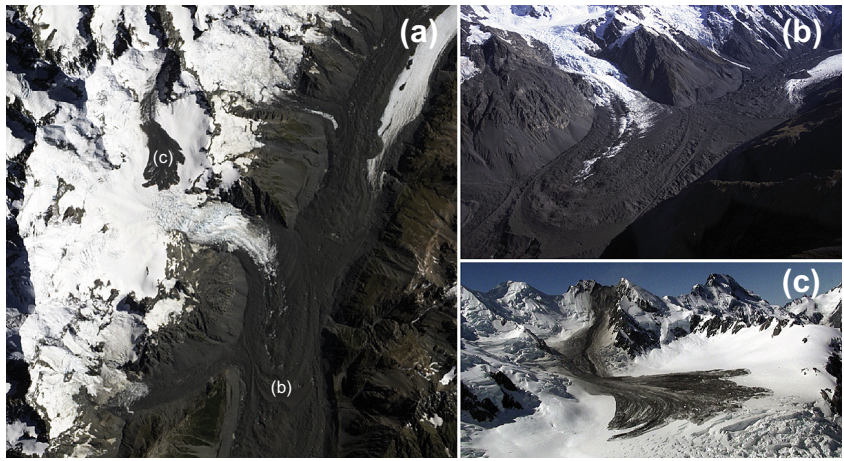

FIGURE 9.12 Rock avalanches in the Aoraki/Mount Cook area, New Zealand. (a) Aoraki/Mount Cook, Tasman Glacier and 1991 and 2013 rock avalanche deposits *(Image: NASA Earth Observatory, J. Allen and R. Simmon, February 5, 2013.)*; (b) transportation of the 1991 Aoraki/Mount Cook rock avalanche deposit through the Hochstetter icefall *(Photo: N. Reznichenko)*; (c) Rock avalanche deposit on Grand Plateau that fell from Mount Dixon in January 2013 *(Photo: Alpine Guides)*.

an average debris thickness of 3–7 m, giving a volume of 0.14–0.20 Mm^3. The debris sat on a pedestal of ice 30–40 m thick (Reznichenko et al., 2011). Thus, in 5 years the rock avalanche protected 1.7 Mm^3 of ice and rock over an area of about 5 ha, or 34 m of ice (Reznichenko et al., 2011). Reported rock avalanches on Hooker Glacier suggest that they fall onto this glacier with about a decadal frequency.

The frequency of these events raises concern about of the hazard for tourist activities around Aoraki/Mount Cook National Park. To date, although there are many eyewitness accounts of rock avalanches (e.g., in 1991, 2004, and 2013) no fatal consequences are reported. However Plateau Hut, which holds tens of climbers most of the summer, was within a few hundred meters of being affected by both the 1991 and 2013 events.

9.4.2 The 1991 Chillinji Glacier Rock Avalanche (Western Karakoram)

A rock avalanche deposit was first observed in the upper ablation zone of Chillinji Glacier, Karambar valley, in June 1992. The landslide material had intact raised rims and distributary lobes, was buried in winter snowfall and showed no modifications by ablation (Figure 9.13(a)). This suggests emplacement in late 1991 or early 1992, possibly traveling over deep winter snow. About a third was buried under avalanche and wind deposited snow, and only revealed by melting in later years. Chillinji is an almost wholly

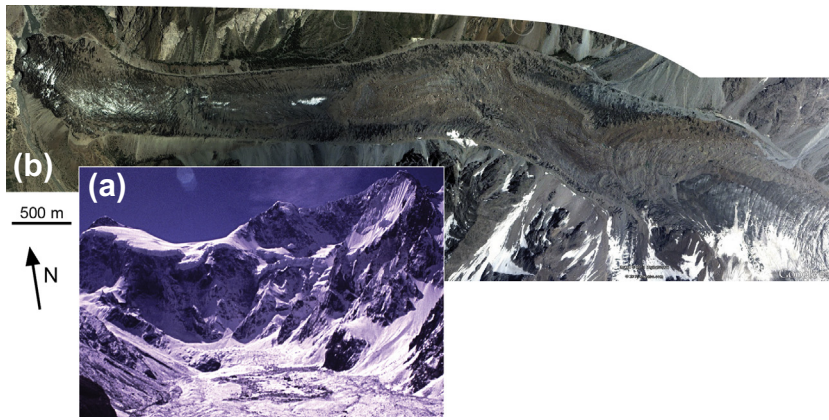

FIGURE 9.13 Chillinji Glacier, Karambar valley, Karakoram. (a) Upper ablation zone of the glacier in June 1992 *(Photo: K. Hewitt)*. (b) The rock avalanche material was still buried in winter snowfall. *Image: Google Earth, 25/07/2009.*

avalanche-nourished glacier or "Turkestan-type" and there are indications it is surge-type (Hewitt, 1998, 2013a).

When revisited in 1994, the rock avalanche area was raised above the surrounding glacier. A steep ice slope 10−20-m-high marked its downglacier edge. Material continually spilled down this slope while most of the rock avalanche deposit above seemed intact and unmodified, suggesting steady transport on the glacier surface. Below the cliff, a broad depression had developed across the glacier. Some 1−2 km further down, radial thickening was observed and, where this reached the glacier margins, ice was overriding the well-defined, tree-covered lateral moraines, indicating accelerated ice movement.

By summer 2009 the front of the rock avalanche debris had been carried 3 km down the glacier (176 m/a). The area of landslide debris had increased from an initial 1.3 km^2 to almost 2 km^2, as upper areas buried in snowpack and snow avalanches had been exhumed (Figure 9.13(b)). An extensive part of the debris had developed what McSaveney (1978) called "transverse folds", ridges and troughs extending radially across the glacier and associated with crevasses of a small icefall. A kilometer further downglacier, there was another, smaller transverse area of heavy debris on the ice, with many large, angular boulders. It seemed to record an older rockslide, possibly a rock avalanche. Rates of movement in this section suggested it was 8−12 years older than the 1991 event.

For some decades before the rock avalanche, and for 14 years afterward, the Chillinji terminus was stationary and a "moraine-dammed" ice tongue with heavy debris cover (Benn et al., 2003). The ice sat on a high ramp of moraine built out into the Karambar valley (Hewitt, 1998). An example of the

Karakoram "Ghulkin-type" of Owen (1994), it resembled the better-known Hatunraju Glacier in the Peruvian Cordillera Blanca (Iturrizaga, 2013), and the Shaigiri Glacier on Nanga Parbat (Kuhle, 1990; Benn et al., 2003). Heavy supraglacial sediment transport was occurring, as was build-up or inefficient removal at the margins.

However, quite suddenly in 2005 the Chillinji tongue broke through the terminal moraine-dam, as a breach-lobe. It advanced about a kilometer diagonally into the Karambar River, moving upvalley to rest against the far wall. Although the rock avalanche debris was 2.5 km from the location of the former, stable terminus and about 3 km from the extended terminus, it seems reasonable to suggest that accelerated ice, observed at the front of the rock avalanche in 1994, involved a kinematic wave that traveled ahead and faster than the landslide debris to reach the terminus first.

The Chillinji has dammed Karambar River in the past, but in this instance and so far, channels have been maintained under the ice (Hewitt, 1998; Hewitt and Liu, 2010). The terminal lobe remains heavily crevassed and debris tumbles down from a cliffed ice-edge and steep moraines into the river. It seems likely this condition will persist over the next several decades and further advance is likely as the thickened area, protected by rock avalanche debris, approaches the terminus. An ice dam could be sealed at some point, threatening GLOFs.

Benn et al. (2003) considered their moraine-dammed, "uncoupled" type to be typical of debris-covered glaciers. Their "outwash-head", "coupled" type is relatively free of surface debris. Change from one to the other type was seen to depend upon climate change. However, Chillinji changed from one to the other while the glacier remained debris-covered, and unrelated to climate. The change was associated with accelerated ice movement reaching the terminus from, but ahead of, the rock avalanche area.

Conditions at Chillinji illustrate how landslides can alter the usual picture of glacial fluctuations and sedimentation regulated by climate. For the past 23 years, and possibly for some decades into the future, the landslide influences glacier dynamics, mass balance, ice-margin conditions, and sedimentation. Its debris alters rates and patterns of glacier ablation, surface elevation, and movement geometry. The patterns, pace, and composition of sediment delivery are altered as landslide material is dispersed and modified by glacial activity. Over the half-century or more required to carry the landslide materials to the ice margin and beyond, they strongly buffer glacier conditions. Behavior is the reverse of what might be expected under present climatic warming—thickening not thinning, advance not retreat, a more vigorous tongue with increased sediment transport and release, not less. Positive mass balance and advance were observed at Chillinji when most glaciers in the western Karakoram and Hindu Raj were retreating or stable (Hewitt, 1998, 2005).

Of course, any broader significance of this event depends on whether the landslide is just an isolated occurrence, or if such events recur with sufficient

frequency to be a perennial influence. Too few glaciers have been investigated to say how typical this case is. However, recently, reports show that rock avalanches descend on glaciers at least once in 2 years across the Greater Karakoram region. If at all representative, that suggests as many as 5,000 such events in the Holocene. If, as seems likely, major concentrations of events occur during and after large earthquakes, there would be many more. The potential of rare megaearthquakes in the NW Himalaya and Hindu Kush may mean recent events underestimate long-term incidence (Feldl and Bilham, 2006; Hough et al., 2009; Hewitt et al., 2011a). Repeated rock avalanches may have greater significance to long-term glacier behavior than has hitherto been considered.

Of course, in Holocene time, Chillinji and other glaciers in the region have not only been responding to rock avalanches. The LIA and other Neoglacial climatic advances were pervasive influences. However, it cannot be taken for granted that all glacial fluctuations are climate markers. And in Karambar Valley, as in much of the region, other conditions affect the sediment assemblages and glacier behavior (Figure 9.14).

First, several of the glaciers involved are known to be of surge-type. These advance, retreat and have mass balance cycles peculiar to the basin concerned, and largely independent of climate (Jiskoot, 2011b). An exceptional concentration of surge-type glaciers occurs in the Karakoram including several with identified rock avalanches (Gardner and Hewitt, 1990; Hewitt, 1998, 2009b).

Second, 10 glaciers, including Chillinji, have tongues that enter the channel of the Karambar River and have dammed it in the past 200 years (Hewitt and Liu, 2010). Even without dams, lateral moraines and other glacial deposits partly close the valley. They change the river's course and sediment transport. Thus, the whole river system is disturbed and fragmented by glacier interference. The main interest here is how rock avalanches from walls in glaciers basins have repeatedly helped control glacial processes (Evans, 2003; Hewitt, 2006, 2013b).

9.4.3 Holocene Horcones Mass Flow, Cerro Aconcagua (6961 m a.s.l.), Argentina

The Horcones deposit has long puzzled, and been disputed by, scientists. This applies, especially, to the great hummocky mass around the confluence of Horcones and Las Cuevas valley in Mendoza Province (Figure 9.15(a)). For some time the deposit had been identified and mapped as Late-Glacial moraine, but others suggested it could be a postglacial landslide deposit from collapsed glaciofluvial deposits. Matters are complicated by the Horcones Glacier being surge-type. It last surged in the 1990s (Figure 9.15(b)).

Resolving the dispute also happens to be of critical importance for hazard assessment of the nearby community of Puente del Inca, on a vital, trans-Andean transportation corridor. Also, the deposit is at the entrance of a

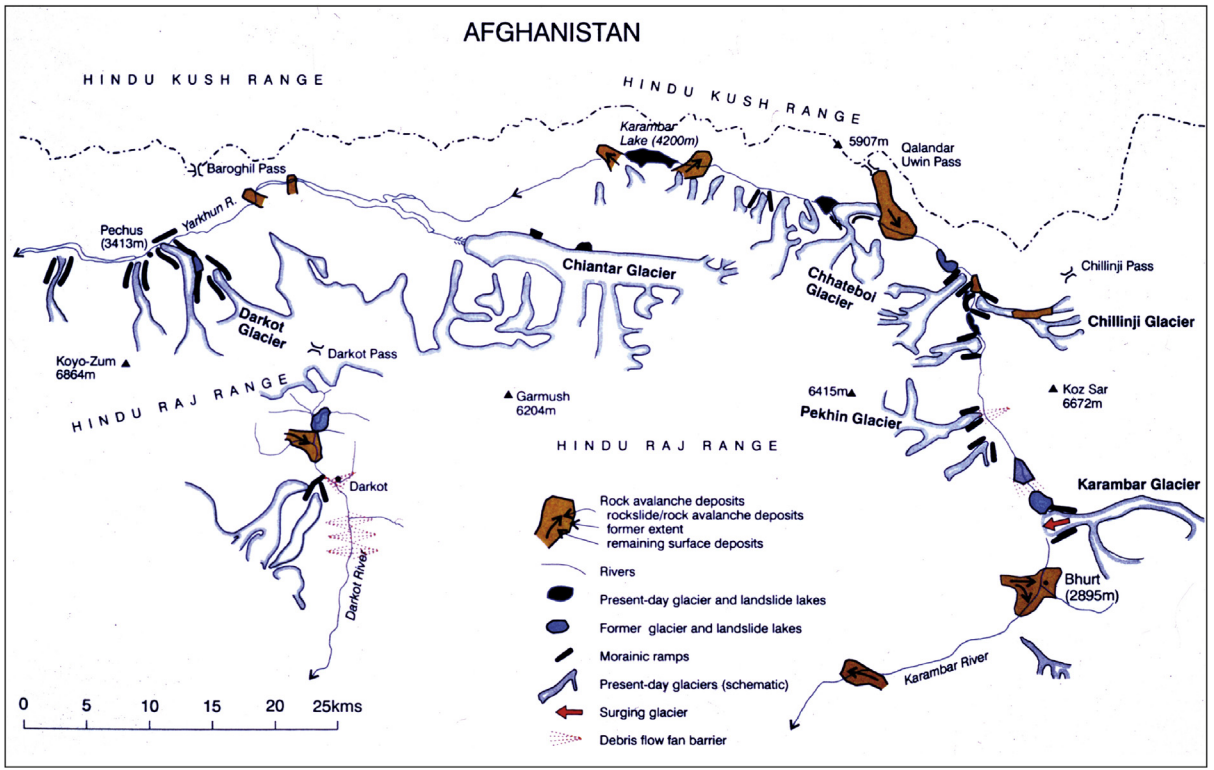

FIGURE 9.14 Glaciers and glacier dams in the Karambar Valley, Karakoram. *After Hewitt, 1998.*

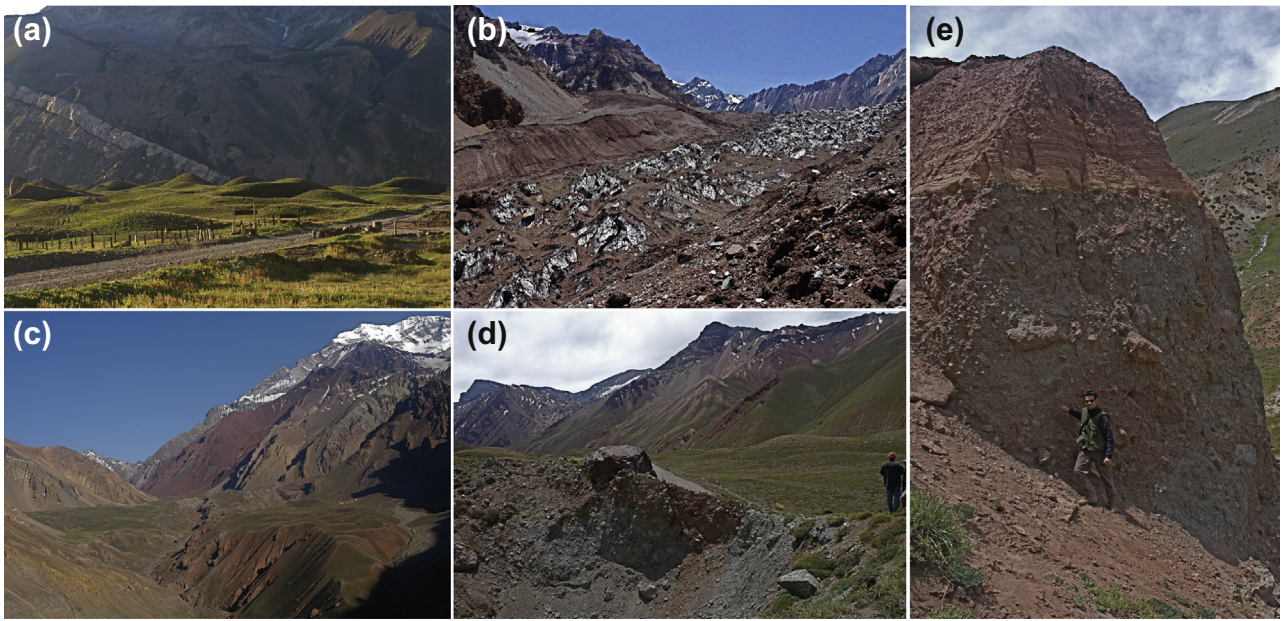

FIGURE 9.15 The Holocene Horcones deposit, Cerro Aconcagua, Argentina. (a) Hummocky surface of the lower Horcones lobe around the junction with Las Cuevas Valley *(Photo: K. Hewitt)*; (b) lower Horcones Glacier shortly after its last surge. Initially the mass flow traveled over the glacier, entraining debris from the conspicuous reddish on-ice and lateral moraines *(Photo: K. Hewitt)*; (c) the Horcones deposit at and below the junction of the Horcones Glacier (enters from the right middle ground, above small park camp site and below Aconcagua Peak, top right) *(Photo: K. Hewitt)*; (d) lower Horcones deposit showing relations of gray and red material, and large boulders in a sink hole, evidently left where an incorporated ice block melted out *(Photo: K. Hewitt)*; (e) terminal area of Horcones deposit in the Las Cuevas valley, showing typical, segregated gray and red materials, and lacustrine beds from the original impoundment by the mass flow *(Photo: K. Hewitt)*.

national park where trekking and mountaineering are expanding. If it is strictly glacial, long periods would be required for the glaciers to grow enough to advance to the critical areas, even with surging. If it is related to a postglacial catastrophic landslide the question is whether conditions could bring a recurrence at any time, here or elsewhere.

A reconstruction, seen as more convincing here, does suggest that the deposit originated in a massive rock slope failure on Cerro Aconcagua. It is thought to have descended onto Horcones Glacier from Cerro Aconcagua as a rockfall—rock avalanche. Like the calamitous Nevados Huascaran landslide in Peru, 1970 (Plafker and Ericksen, 1978), large quantities of ice and snow that were part of the Horcones event may have come with the original mass failure on the peak. However some or most may have been picked up during its runout, along with additional debris, including moraine deposits scooped up from the Horcones Glacier margins and forefield. All of this contributed to a megaslide of more than 3 km^3 (Fauqué et al., 2009). During runout, it was transformed into a saturated mass flow and traveled another 8 km beyond the glacier terminus, to dam the main Las Cuevas valley, where the Trans-Andean Highway is located today.

Beyond the Horcones snout, at the junction of three valleys, the deposit separated into lobes entering each one, but the largest turned through 90° to descend the main valley. Morphology here is also hummocky; there were run-ups of over 100 m on slopes round the bend in the valley (Figure 9.15(c)). In the upper end of the valley below Horcones Glacier the deposit is composed of a single lithology from Cerro Aconcagua south face; a gray material mineralogically distinct from lateral moraine deposits of the last glaciation, and whose clasts are very angular and internally fractured. Reddish material is conspicuous below the junction and on the left flank of the valley.

There is a gap in the narrow, steeper gorge between the upper and lower main deposits, with no landslide material evident. Possibly this is due to subsequent erosion in the gorge, possibly to an acceleration of the flow here that carried most or all of the debris through the section. Rheological differences in the largest, lower mass may also be a factor; this is a hummocky deposit emplaced up to 20 km from Cerro Aconcagua, filling the lower 4 km valley floor. The lowest section has most intrigued and puzzled scientists. It is tens of meters thick, higher at midvalley than the margins and consists largely of thoroughly crushed and broken, gray rock of the Cerro Aconcagua lithology. However, many inclusions of red material occur as well, with subangular to subrounded clasts of various lithologies that outcrop along the Horcones valley and are found as the main components of lateral moraines there. In the deposits, boundaries between the two materials are sharp. They do not mix, although complexly contorted and intertwined in the mass (Figure 9.15(d)). Lacustrine beds over the landslide materials record how it dammed the Cuevas River for some decades or centuries (Figure 9.15(e)).

Age determinations for the mass flow by ^{36}Cl surface exposure dating vary between 8,800 and 11,100 years (Fauqué et al., 2009). The overlapping variations are possibly due to provenance and remnant ages in prelandslide materials, possibly sampling and technical uncertainties and conceivably more than one event. Some ^{14}C ages of underlying fluvial deposits are around 12,640 year BP. The same interval is identified by the lake sediments in the Las Cuevas valley (13,670–9,180 cal year BP). At least, these ages bracket events since the last major glaciation not, as previously assumed, Late-Glacial ones. Other rock avalanche deposits have been identified in adjacent valleys, and at least one has similar characteristics and age to the Horcones deposit. Postglacial climatic conditions, paraglacial adjustment of rock slopes, and earthquake activity may have been preparatory or triggering factors. Fauqué et al. (2009) suspected that climate warming could lead to similar events in future.

9.5 CONCLUSIONS

Rock avalanches can bring some of the most drastic and rapid changes in mountain landscapes, especially when they travel onto glaciers, where their velocity decreases more slowly than it would over ice free terrain, and their volume grows through incorporation of ice and supraglacial debris. Various preparatory factors, from glacier erosion, thinning and retreat, to earthquakes and permafrost degradation can act to destabilize rockwalls in glaciated, or formerly glaciated, basins. The forces unleashed in the rock avalanche, and the danger that some can continue past the glacier terminus into inhabited areas, make them highly threatening processes.

In most mountains landslide frequency is poorly documented, although new teleseismic techniques are facilitating their identification in remote areas. Further, rock avalanche deposits have commonly been confused with other, similar ones, especially in glacier environments, but new techniques promise to unequivocally identify rock avalanche deposits in the future.

Finally, the risks from these events are growing in many of mountain areas, due to greater populations, infrastructure, facilities, and activities. The problem is often not even recognized or, in cases where landslides have been misinterpreted as due to other processes, especially pre-Holocene glaciations, are assumed to represent other, less significant geohazards.

REFERENCES

Aeschlimann, H., 1983. Zur Gletschergeschichte des italienischen Mont Blanc Gebietes: Val Veni – Val Ferret – Ruitor (Ph.D. thesis). Universität Zürich, 105 pp.

Agassiz, L., 1845. Les glaciers et le terrain erratique du revers méridional du Mont-Blanc. In: Desor, E. (Ed.), Nouvelles excursions et séjours dans les glaciers et les hautes régions des Alpes de M. Agassiz et de ses compagnons de voyage. Kissling, Neuchâtel, 266 pp.

Akçar, N., Deline, P., Ivy-Ochs, S., Alfimov, V., Hajdas, I., Kubik, P.W., Christl, M., Schlüchter, C., 2012. The AD 1717 rock avalanche deposits in the upper Ferret Valley (Italy): a dating approach with cosmogenic ^{10}Be. J. Quat. Sci. 27, 383–392. http://dx.doi.org/10.1002/jqs.1558.

Akçar, N., Deline, P., Ivy-Ochs, S., Alfimov, V., Kubik, P.W., Christl, M., Schlüchter, C., 2014. Minor inheritance inhibits the calibration of the ^{10}Be production rate from the AD 1717 Val Ferret rock avalanche, European Alps. J. Quat. Sci. 29, 318–328. http://dx.doi.org/10.1002/jqs.2706.

Alexander, Davies, D.J., T.R.H., Shulmeister, J., 2014. Formation and evolution of the Waiho Loop terminal moraine New Zealand. J. Quat. Sci. 29 (4), 361–369. http://dx.doi.org/10.1002/jqs.2707.

Allen, S.K., Cox, S.C., Owens, I.F., 2011. Rock avalanches and other landslides in the central Southern Alps of New Zealand: a regional study considering possible climate change impacts. Landslides 8, 33–48.

Applegate, P.J., Lowell, T.V., Alley, R.B., 2008. Comment on "Absence of cooling in New Zealand and the adjacent ocean during the Younger Dryas chronozone". Science 320, 746.

Barff, E., 1873. A letter respecting the recent change in the apex of Mount Cook communicated by J. Hector. Trans. Proc. N. Z. Inst. 6, 379–380.

Barrows, T.T., Lehman, S.J., Fifield, L.K., De Deckker, P., 2008. Absence of cooling in New Zealand and the adjacent ocean during the Younger Dryas chronozone. Science 318, 86–89.

Benn, D., Kirkbride, M.P., Owen, L.A., Brazier, V., 2003. Glaciated valley landsystems. In: Evans, D.J.A. (Ed.), Glacial Landsystems. Hodder Arnold, London, pp. 372–406.

Boulton, G.S., 1978. Boulder shapes and grain-size distributions of debris as indicators of transport paths through a glacier and till genesis. Sedimentology 25, 773–799.

Collins, G.S., Melosh, H.J., 2003. Acoustic fluidization and the extraordinary mobility of sturzstroms. J. Geophys. Res. Solid Earth 108.

Cook, S.J., Porter, P.R., Bendall, C.A., 2013. Geomorphological consequences of a glacier advance across a paraglacial rock avalanche deposit. Geomorphology 189, 109–120.

Cossart, E., Braucher, R., Fort, M., Bourlés, D.L., Carcaillet, J., 2008. Slope instability in relation to glacial debuttressing in alpine areas (Upper Durance catchment, southeastern France): evidence from field data and ^{10}Be cosmic ray exposure ages. Geomorphology 95, 3–26.

Cox, S.C., Ferris, B.G., Allen, S., 2008. Vampire rock avalanches, Aoraki/Mount Cook National Park, New Zealand. In: GNS Science Report 2008.10, 34 pp.

Crandell, D.R., Fahnestock, R.K., 1965. Rockfalls and Avalanches from Little Tahoma Peak on Mount Rainier. U.S. Geological Survey Bulletin, 1221-A, Washington, 30 pp.

Crosta, G.B., Frattini, P., Fusion, N., 2007. Fragmentation in the Val Pola rock avalanche, Italian Alps. J. Geophys. Res. 112, F01006. http://dx.doi.org/10.1029/2005JF000455.

Davies, T.R.H., 1982. Spreading of rock avalanche debris by mechanical fluidization. Rock Mech. 15, 9–24.

Davies, T.R.H., 2013. Fluvial processes in proglacial environments. In: Shroder, J.F. (Ed.), Treatise on Geomorphology, vol. 8. Academic Press, San Diego, pp. 141–150.

Davies, M.C.R., Hamza, O., Harris, C., 2001. The effect of rise in mean annual temperature on the stability of rock slopes containing ice-filled discontinuities. Permafrost Periglac. 12, 137–144.

Davies, T.R.H., McSaveney, M.J., 1999. Runout of dry granular avalanches. Can. Geotech. J. 36, 313–320.

Davies, T.R.H., McSaveney, M.J., 2002. Dynamic simulation of the motion of fragmenting rock avalanches. Can. Geotech. J. 39, 789–798.

Davies, T.R.H., McSaveney, M.J., 2009. The role of rock fragmentation in the motion of large landslides. Eng. Geol. 109, 67–79.

Davies, T.R.H., McSaveney, M.J., 2012. Mobility of long-runout rock avalanches. In: Clague, J.J., Stead, D. (Eds.), Landslides: Types, Mechanisms and Modeling. Cambridge University Press, pp. 50–58.

Davies, T.R.H., McSaveney, M.J., Hodgson, K.A., 1999. A fragmentation-spreading model for long-runout rock avalanches. Can. Geotech. J. 36, 1096–1110.

Davies, T.R.H., McSaveney, M.J., Kelfoun, K., 2010. Runout of the Socompa volcanic debris avalanche, Chile: a mechanical explanation for low basal shear resistance. Bull. Volcanol. 72, 933–944. http://dx.doi.org/10.1007/s00445-010-0372-9.

Decaulne, A., Sæmundsson, þ., Pétursson, H.G., Jónsson, H.P., Sigurðsson, I.A., 2010. A large rock avalanche onto Morsarjökull Glacier, South-East Iceland. Its implications, or Ice-surface evolution and glacier dynamic. In: Iceland in the Central Northern Atlantic: Hotspot, Sea Currents and Climate Change, Plouzané, France hal-00482107.

Deline, P., 2001. Recent Brenva rock avalanches (Valley of Aosta): new chapter in an old story? Geogr. Fis. Din. Quat. 5 (Suppl.), 55–63.

Deline, P., 2009. Interactions between rock avalanches and glaciers in the Mont Blanc massif during the late Holocene. Quat. Sci. Rev. 28, 1070–1083. http://dx.doi.org/10.1016/j.quascirev.2008.09.025.

Deline, P., Kirkbride, M.P., 2009. Rock avalanches on a glacier and morainic complex in Haut Val Ferret (Mont Blanc massif, Italy). Geomorphology 103, 80–92. http://dx.doi.org/10.1016/j.geomorph.2007.10.020.

Denton, G.H., Hendy, C.H., 1994. Younger Dryas age advance of Franz Josef Glacier in the Southern Alps of New Zealand. Science 264, 1434–1437.

Dunning, S.A., 2004. Rock Avalanches in High Mountains (Ph.D. thesis). University of Luton, 309 pp.

Dutto, F., Mortara, G., 1991. Grandi frane storiche con percorso su ghiacciao in Valle d'Aosta. Rev. Valdôtaine Hist. Nat. 45, 21–35.

Dufresne, A., Davies, T.R.H., 2009. Longitudinal ridges in mass movement deposits. Geomorphology 105, 171–181.

Eberhardt, E., Stead, D., Coggan, J.S., 2004. Numerical analysis of initiation and progressive failure in natural rock slopes – the 1991 Randa rockslide. Int. J. Rock Mech. Min. Sci. 41, 69–87.

Eisbacher, G.H., Clague, J.J., 1984. Destructive mass movements in high mountains: hazard and management. Geol. Surv. Can. Pap. 84-16, 230 pp.

Ekstrom, G., Stark, C.P., 2013. Simple scaling of catastrophic landslide dynamics. Science 339, 1416–1419.

Evans, D.J.A. (Ed.), 2003. Glacial Landsystems. Hodder Arnold, London, 532 pp.

Evans, D.J.A., Rea, H.R., 2003. Surging glacier landsystem. In: Evans, D.J.A. (Ed.), Glacial Landsystems. Hodder Arnold, London, pp. 259–288.

Evans, S.G., Clague, J.J., 1994. Recent climatic change and catastrophic geomorphic processes in mountain environments. Geomorphology 10, 107–128.

Evans, S.G., Clague, J.J., 1988. Catastrophic rock avalanches in glacial environments. In: Bonnard, C. (Ed.), Proceedings of the 5th International Symposium on Landslides, vol. 2. Balkema, Rotterdam, pp. 1153–1158.

Evans, S.G., Clague, J.J., 1998. Rock avalanche from Mount Munday, Waddington Range, British Columbia, Canada. Landslide News 11, 23–25.

Evans, S.G., Clague, J.J., 1999. Rock avalanches on glaciers in the Coast and St. Elias Mountains, British Columbia. In: Proceedings of the 13th Annual Vancouver Geotechnical Society Symposium, Vancouver, pp. 115–123.

Evans, S.G., Bishop, N.F., Smoll, L.F., Valderrama Murillo, P., Delaney, K.B., Oliver-Smith, A., 2009a. A Re-Examination of the Mechanism and Human Impact of Catastrophic Mass Flows Originating on Nevado Huascarán, Cordillera Blanca, Peru in 1962 and 1970. Eng. Geology 108, 96–118.

Evans, S.G., Tutubalina, O.V., Drobyshev, V.N., Chernomorets, S.S., McDougall, S., Petrakov, D.A., Hungr, O., 2009b. Catastrophic detachment and high-velocity long-runout flow of Kolka Glacier, Caucasus Mountains, Russia in 2002. Geomorphology 105, 314–321.

Eyles, N., Rogerson, R.J., 1978. A framework for the investigation of medial moraine formation: Austerdalsbreen, Norway, and Berendon Glacier, British Columbia, Canada. J. Glaciol. 20, 99–113.

Fahnestock, R.K., 1978. Little Tahoma Peak rockfalls and avalanches. Mount Rainier, Washington, U.S.A.. In: Voight, B. (Ed.), Rockslides and avalanches, 1 Natural phenomena. Elsevier, Amsterdam, pp. 181–196.

Fauqué, L., Hermanns, R., Hewitt, K., Rosas, M., Wilson, C., Baumann, V., Lagorio, S., Di Tommaso, I., 2009. Mega-deslizamientos de la pared sur del Cerro Aconcagua y su relación con depósitos asignados a la glaciación pleistocena. Rev. Asoc. Geol. Argent. 65, 691–712.

Feldl, N., Bilham, R., 2006. Great Himalayan earthquakes and the Tibetan Plateau. Nature 444, 165–170. http://dx.doi.org/10.1038/nature05199.

Fischer, L., Kääb, A., Huggel, C., Noetzli, J., 2006. Geology, glacier retreat and permafrost degradation as controlling factors of slope instabilities in a high-mountain rock wall: Monte Rosa east face. Nat. Hazards Earth Syst. Sci. 6, 761–772.

Fountain, A.G., Jacobel, R.W., Schlichting, R., Jansson, P., 2005. Fractures as the main pathways of water flow in temperate glaciers. Nature 433, 618–621.

Friedmann, S.J., 1997. Rock avalanches of the Miocene Shadow Valley basin, eastern Mojave Desert, California: processes and problems. J. Sediment. Res. 67a, 792–804.

Fort, M., Cossart, E., Deline, P., Dzikowski, M., Nicoud, G., Ravanel, L., Schoeneich, P., Wassmer, P., 2009. Geomorphic impacts of large and rapid mass movements; a review. Géomorphol. Relief Processus Environ. 1, 47–64.

Gardner, J.S., Hewitt, K., 1990. A surge of Bualtar Glacier, Karakoram Range, Pakistan – a possible landslide trigger. J. Glaciol. 36, 159–162.

Geertsema, M., 2012. Initial observations of the 11 June 2012 Rock/Ice Avalanche, Lituya Mountain, Alaska. In: Wei, S., Ying, G., Chengcheng, Z. (Eds.), Proceedings of the First Meeting of Cold Region Landslides Network (International Consortium on Landslides). Harbin, pp. 49–53.

Geertsema, M., Clague, J.J., Schwab, J.W., Evans, S.G., 2006. An overview of recent large catastrophic landslides in northern British Columbia, Canada. Eng. Geol. 83, 120–143.

Giani, G.P., Silvano, S., Zanon, G., 2001. Avalanche of 18 January 1997 on Brenva Glacier, Mont Blanc Group, Western Italian Alps: an unusual process of formation. Ann. Glaciol. 32, 333–338.

Gordon, J.E., Birnie, R.V., Timmis, R., 1978. A major rockfall and debris slide on the Lyell Glacier, South Georgia. Arct. Alp. Res. 10, 49–60.

Gruber, S., Haeberli, W., 2007. Permafrost in steep bedrock slopes and its temperature-related destabilization following climate change. J. Geophys. Res. 112, F02S18. http://dx.doi.org/10.1029/2006JF000547.

Gruber, S., Hoelzle, M., Haeberli, W., 2004. Permafrost thaw and destabilization of Alpine rock walls in the hot summer of 2003. Geophys. Res. Lett. 31, L13504. http://dx.doi.org/10.1029/2004GL020051.

Guthrie, R.H., Friele, P., Allstadt, K., Roberts, N., Evans, S.G., Delaney, K.B., Roche, D., Clague, J.J., Jakob, M., 2012. The 6 August 2010 Mount Meager rock slide-debris flow, Coast Mountains, British Columbia: characteristics, dynamics, and implications for hazard and risk assessment. Nat. Hazards Earth Syst. Sci. 12, 1–18. http://dx.doi.org/10.5194/nhess-12-1-2012.

Haeberli, W., Wegmann, M., Vonder Mühll, D., 1997. Slope stability problems related to glacier shrinkage and permafrost degradation in the Alps. Eclogae Geol. Helv. 90, 407–414.

Haeberli, W., Kääb, A., Paul, F., Chiarle, M., Mortara, G., Mazza, A., Deline, P., Richardson, S., 2002. A surge-type movement at Ghiacciaio del Belvedere and a developing slope instability in the east face of Monte Rosa, Macugnaga, Italian Alps. Norw. J. Geogr. 56, 104–111.

Hasler, A., Gruber, S., Font, M., Dubois, A., 2011. Advective heat transport in frozen rock clefts – conceptual model, laboratory experiments and numerical simulation. Permafrost Periglac. 22, 378–389.

Heim, A., 1932. Bergsturz und Menschenleben. Frets und Wasmuth, Zürich, 218 pp.

Heinrichs, T.A., Mayo, L.R., Trabant, D., March, R., 1995. Observations of the surge-type Black Rapids Glacier, Alaska, during a quiescent period, 1970–92. U. S. Geol. Surv. Open File 94-512, 131 pp.

Herreid, S.J., Arendt, A.A., Hock, R., Kienholz, C., 2010. A New Inventory of Glaciers and Supraglacial Debris for the Alaska Range with a Case Study of Rock Avalanche Loading. AGU Fall Meeting, San Francisco.

Hewitt, K., 1988. Catastrophic landslide deposits in the Karakoram Himalaya. Science 242, 64–67.

Hewitt, K., 1998. Himalayan Indus streams in the Holocene: glacier-, and Landslide-'Interrupted' fluvial systems. In: Stellrecht, I. (Ed.), Karakorum-Hindu Kush-Himalaya: Dynamics of Change Part I. Rudiger Koppe Verlag, Koln, pp. 1–28.

Hewitt, K., 1999. Quaternary moraines vs catastrophic rock avalanches in the Karakoram Himalaya, Northern Pakistan. Quat. Res. 51, 220–237.

Hewitt, K., 2002. Styles of rock avalanche depositional complex in very rugged terrain, Karakoram Himalaya, Pakistan. In: Evans, S.G., DeGraff, J.V. (Eds.), Catastrophic Landslides: Effects, Occurrence, and Mechanisms, Reviews in Engineering Geology. Geological Society of America, Boulder, pp. 345–378.

Hewitt, K., 2005. The Karakoram Anomaly? Glacier expansion and the 'elevation effect', Karakoram Himalaya, Inner Asia. Mt. Res. Dev. 25, 332–348.

Hewitt, K., 2006. Disturbance regime landscapes: mountain drainage systems interrupted by large rockslides. Prog. Phys. Geogr. 30, 365–393.

Hewitt, K., 2009. Rock avalanches that travel onto glaciers: disturbance regime landscapes, Karakoram Himalaya, Inner Asia. Geomorphology 103, 66–79.

Hewitt, K., 2013a. Glaciers of the Karakoram Himalaya: Glacial Environments, Processes, Hazards and Resources. Springer, Heidelberg, 363 pp.

Hewitt, K., 2013b. The Great Lateral Moraine, Karakoram Himalaya, Inner Asia. Geogr. Fis. Din. Quat. 36, 1–14. http://dx.doi.org/10.4461/Gfdq.2013.36.0.

Hewitt, K., Clague, J.J., Orwin, J., 2008. Legacies of catastrophic rock slope failures in mountain landscapes. Earth Sci. Rev. 87, 1–38.

Hewitt, K., Liu, J., 2010. Ice-dammed lakes and outburst floods, Karakoram Himalaya: historical perspectives and emerging threats. Phys. Geogr. 31, 528–551.

Hewitt, K., Clague, J.J., Gosse, J., 2011a. Rock avalanches and the pace of late Quaternary development of river valleys in the Karakoram Himalaya. Geol. Soc. Am. Bull. 123, 1836–1850.

Hewitt, K., Clague, J.J., Deline, P., 2011b. Catastrophic rock slope failures and mountain glaciers. In: Singh, V.P., Singh, P., Haritashaya, U.K. (Eds.), Encyclopaedia of Snow, Ice and Glaciers. Springer, Dordrecht, pp. 112–126.

Hochstein, M.P., Claridge, D., Henrys, S.A., Pyne, A., Nobes, D.C., Leary, S.F., 1995. Downwasting of the Tasman Glacier, South Island, New Zealand: changes in the terminus region between 1971 and 1993. N. Z. J. Geol. Geophys. 38, 1–16.

Hough, S., Bilham, R., Bhat, I., 2009. Kashmir Valley megaearthquakes. Am. Sci. 97, 42–49. http://dx.doi.org/10.1511/2009.76.1.

Hsü, K.J., 1975. Catastrophic debris streams (sturzstroms) generated by rockfalls. Geol. Soci. Am. Bull. 86, 129–140.

Huggel, C., 2008. Recent extreme slope failures in glacial environments: effects of thermal perturbation. Quat. Sci. Rev. 28, 1119–1130.

Huggel, C., Zgraggen-Oswald, S., Haeberli, W., Kaab, A., Polkvoi, A., Galushkin, I., Evans, S.G., 2005. The 2002 rock/ice avalanche at Kolka/Karmadon, Russian Caucasus: assessment of extraordinary avalanche formation and mobility, and application of QuickBird satellite imagery. Nat. Hazards Earth Sys. Sci. 5, 173–187.

Huggel, C., Caplan-Auerbach, J., Waythomas, C.F., Wessels, R.L., 2007. Monitoring and modeling ice-rock avalanches from ice-capped volcanoes: a case study of frequent large avalanches on Iliamna Volcano, Alaska. J. Volcanol. Geotherm. Res. 168, 114–136.

Huggel, C., Caplan-Auerbach, J., Gruber, S., Molnia, B., Wessels, R., 2008. The 2005 Mt. Steller, Alaska, rock–ice avalanche: a large slope failure in cold permafrost. In: Kane, D.L., Hinkel, K.M. (Eds.), Proceedings of the 9th International Conference on Permafrost. Alaska, Fairbanks, pp. 747–752.

Imhof, P., 2010. Glacier Fluctuations in the Italian Mont Blanc Massif from the Little Ice Age until the Present. Historical Reconstructions for the Miage, Brenva and Pré-de-Bard Glaciers (MSc thesis). Universität Bern, 132 pp.

Iturrizaga, L., 2006. Transglacial landforms in the Karakoram (Pakistan): a case study from Shimshal Valley. In: Kreutzmann, H. (Ed.), Karakoram in Transition: Culture, Development and Ecology in the Hunza Valley. Oxford University Press, Karachi, 419 pp.

Iturrizaga, L., 2013. Bent glacier tongues: a new look at Lliboutry's model of the evolution of the crooked Jatunraju Glacier (Parón Valley, Cordillera Blanca, Perú). Geomorphology 198, 147–162.

Jibson, R.W., Harp, E.L., Schulz, W., Keefer, D.K., 2006. Large rock avalanches triggered by the M 7Æ9 Denali Fault, Alaska, earthquake of 3 November 2002. Eng. Geol. 83, 144–160.

Jiskoot, H., 2011a. Long-runout rockslide on glacier at Tsar Mountain, Canadian Rocky Mountains: potential triggers, seismic and glaciological implications. Earth Surf. Processes Landforms 36, 203–216.

Jiskoot, H., 2011b. Glacier surging. In: Singh, V.P., Singh, P., Haritashaya, U.K. (Eds.), Encyclopaedia of Snow, Ice and Glaciers. Springer, Dordrecht, pp. 415–428.

Johnson, N.M., Ragle, R.H., 1968. Analysis of Flow Characteristics of Allen II Slide from Aerial Photographs, the Great Alaska Earthquake of 1964-Hydrology, Part A. National Academy of Sciences, Washington, D.C, 369–373.

Kjartansson, G., 1967. The Steinsholtshlaup, central-south Iceland on January 15th, 1967. Jökull 17, 249–262.

Keefer, D.K., 1984. Rock avalanches caused by earthquakes: source characteristics. Science 223, 1288–1290.

Keefer, D.K., 1999. Earthquake-induced landslides and their effects on alluvial fans. J. Sediment. Res. 69, 84–104.

Keefer, D.K., 2002. Investigating landslides caused by earthquakes – a historical review. Surv. Geophys. 23, 473–510.

Kent, P.E., 1966. The transport mechanism in catastrophic rock falls. J. Geol. 74, 79–83.

Kirkbride, M.P., Sugden, D., 1992. New Zealand loses its top. Geogr. Mag. 64, 30–34.

Kirkbride, M.P., Winkler, S., 2012. Correlation of Late Quaternary moraines: impact of climate variability, glacier response, and chronological resolution. Quat. Sci. Rev. 46, 1–29.

Kotlyakov, V.M., Rototaeva, O.V., Nosenko, G.A., 2004a. The September 2002 Kolka Glacier catastrophe in North Ossetia, Russian Federation: evidence and analysis. Mt. Res. Dev. 24, 78–83.

Kotlyakov, V.M., Rototaeva, O.V., Desinov, L.V., Zotikov, I.A., Osokin, N.I., 2004b. Causes and effect of a catastrophic surge of Kolka glacier in the Central Caucasus. Z. Gletscherkd. Glazialgeol. 38, 117–128.

Kuhle, M., 1990. Ice marginal ramps and alluvial fans in semiarid mountains: convergence and difference. In: Rachocki, A.H., Church, M. (Eds.), Alluvial Fans: A Field Approach. Wiley, Chichester, pp. 55–68.

Larsen, S., Davies, T.R.H., McSaveney, M.J., 2005. A possible coseismic landslide origin of late Holocene moraines of the Southern Alps, New Zealand. N. Z. J. Geol. Geophys. 48, 311–314.

Lee, E.M., Jones, D.K.C., 2004. Landslide Risk Management. Thomas Telford Publishing, London, 464 pp.

Lipovsky, P.S., Evans, S.G., Clague, J.J., Hopkinson, C., Couture, R., Bobrowsky, P., Ekström, G., Demuth, M.N., Delaney, K.B., Roberts, N.J., Clarke, G., Schaeffer, A., 2008. The July 2007 rock and ice avalanches at Mount Steele, St. Elias Mountains, Yukon, Canada. Landslides 5, 445–455. http://dx.doi.org/10.1007/s10346-008-0133-4.

Malamud, B.D., Turcotte, D.L., Guzzetti, F., Reichenbach, P., 2004. Landslides, earthquakes, and erosion. Earth Planet. Sci. Lett. 229, 45–59.

Mauthner, T.E., 1996. Kshwan Glacier rock avalanche, Southeast of Stewart, British Columbia. Geol. Surv. Can. Curr. Res. 1996-A, 37–44.

Matsuoka, N., Murton, J., 2008. Frost weathering: recent advances and future directions. Permafrost Periglac. 19, 195–210. http://dx.doi.org/10.1002/ppp.620.

Mayr, F., 1969. Die postglazialen Gletscherschwankungen des Mont Blanc-Gebietes. Z. Geomorphol. Suppl. Band 8, 31–57.

McColl, S.T., 2012. Paraglacial rock-slope stability. Geomorphology 153–154, 1–16.

McColl, S.T., Davies, T.R.H., 2011. Evidence for a rock-avalanche origin for the Hillocks moraine, Otago, New Zealand. Geomorphology 127 (3–4), 216–224.

McColl, S.T., Davies, T.R.H., 2013. Large ice-contact slope movements; glacial buttressing, deformation and erosion. Earth Surf. Processes Landforms 38, 1102–1115. http://dx.doi.org/10.1002/esp.3346.

McColl, S.T., Davies, T.R.H., McSaveney, M.J., 2010. Glacier retreat and rock-slope stability: debunking debuttressing. In: Williams, A.L., Pinches, G.M., Chin, C.Y., McMorran, T.J., Massey, C.I. (Eds.), Geologically Active. Taylor and Francis, London, pp. 467–474.

McColl, S.T., Davies, T.R.H., McSaveney, M.J., 2012. The effect of glaciation on the intensity of seismic ground motion. Earth Surf. Processes Landforms 37, 1290–1301. http://dx.doi.org/10.1002/esp.3251/full.

McSaveney, M.J., 1978. Sherman Glacier rock avalanche, Alaska, U.S.A. In: Voight, B. (Ed.), Rockslides and Avalanches, 1. Natural Phenomena. Elsevier, Amsterdam, pp. 197–258.

McSaveney, M.J., 1993. Rock avalanches of 2 May and 16 September 1992, Mount Fletcher, New Zealand. Landslides News 7, 32–34.

McSaveney, M., 2002. Recent rock falls and rock avalanches in Mount Cook National Park, New Zealand. In: Evans, S.G., DeGraff, J.V. (Eds.), Catastrophic Landslides: Effects, Occurrence, and Mechanisms, Reviews in Engineering Geology, vol. 15, pp. 35–70.

McSaveney, M.J., Davies, T.R., 2007. Rockslides and their motion. In: Sassa, K., Fukuoka, H., Wang, F., Wang, G. (Eds.), Progress in Landslide Science. Springer, Berlin, pp. 113–133.

Melosh, H.J., 1979. Acoustic fluidization: a new geologic process? J. Geophys. Res. 84, 7513–7520.

Mihalcea, C., Brock, B.W., Diolaiuti, G., D'Agata, C., Citterio, M., Kirkbride, M.P., Cutler, M.E.J., Smiraglia, C., 2007. Supraglacial surface temperature from ASTER and ground-based measurements analysed to investigate debris-covered pattern on Miage Glacier (Mont Blanc, Italy). Cold Reg. Sci. Technol. 52, 341–354.

Muravyev, Y.D., 2004. Subglacial geothermal eruption – the possible reason of catastrophic surge of Kolka Glacier in Kazbek volcanic massif (Caucasus), bulletin of Kamchatka regional association "Educational-Scientific Center". Earth Sci. 4, 6–20.

Nagai, H., Fujita, K., Nuimura, T., Sakai, A., 2013. Southwest-facing slopes control the formation of debris-covered glaciers in the Bhutan Himalaya. The Cryosphere 7, 1303–1314. http://dx.doi.org/10.5194/tc-7-1303-2013.

Nakawo, M., Rana, B., 1999. Estimate of ablation rate of glacier ice under a supraglacial debris layer. Geogr. Ann. 81A, 695–701.

Nakawo, M., Raymond, C.F., Fountain, A., 2000. Debris-Covered Glaciers. International Association of Hydrological Sciences Publication 264, Wallingford, 288 pp.

Nussbaumer, S.U., Zumbühl, H.J., Steiner, D., 2007. Fluctuations of the Mer de Glace (Mont Blanc area, France) AD 1500–2050: an interdisciplinary approach using new historical data and neural network simulations. Z. Gletscherkd. Glazialgeol. 40 (2005/2006), 1–183.

Orombelli, G., Porter, S.C., 1988. Boulder deposit of upper Val Ferret (Courmayeur, Aosta valley): deposit of a historic giant rockfall and debris avalanche or a late-glacial moraine? Eclogae Geol. Helv. 81, 365–371.

Owen, L., 1994. Glacial and non-glacial diamictons in the Karakoram Mountains and Western Himalaya. In: Warren, W.P., Croots, D. (Eds.), The Formation and Deformation of Glacial Deposits. Balkema, Rotterdam, pp. 9–24.

Pacione, M., 1999. Applied Geography: Principles and Practice. Routledge, London, 664 pp.

Petrakov, D.A., Chernomorets, S.S., Evans, S.G., Tutubalina, O.V., 2008. Catastrophic glacial multi-phase mass movements: a special type of glacial hazard. Adv. Geosci. 14, 211–218.

Pirulli, M., 2009. The Thurwieser rock avalanche (Italian Alps): description and dynamic analysis. Eng. Geol. 109, 80–92. http://dx.doi.org/10.1016/j.enggeo.2008.10.007.

Plafker, G., Ericksen, F.E., 1978. Nevados huascaran avalanches, Peru. In: Voight, B. (Ed.), Rockslides and Avalanches. 1 Natural Phenomena. Elsevier, Amsterdam, pp. 277–314.

Porter, S.C., Orombelli, G., 1980. Catastrophic rockfall of September 12, 1717 on the Italian flank of the Mont Blanc massif. Z. Geomorphol. 24, 200–218.

Porter, S.C., Orombelli, G., 1981. Alpine rockfall hazards. Recognition and dating of rockfall deposits in the western Italian Alps lead to an understanding of the potential hazards of giant rockfalls in mountainous regions. Am. Sci. 69, 67–75.

Post, A., 1967. Effects of the March 1964 Alaska earthquake on glaciers. U.S. Geol. Surv. Prof. Pap. 544-D, 42.

Prager, C., Ivy-Ochs, S., Ostermann, M., Synal, H.-A., Patzelt, G., 2009. Geology and radiometric ^{14}C-, ^{36}Cl- and Th-/U-dating of the Fernpass rockslide (Tyrol, Austria). Geomorphology 103, 93–103.

Putnam, A.E., Denton, G.H., Schaefer, J.M., Barrell, D.J.A., Andersen, B.G., Finkel, R.C., Schwartz, R., Doughty, A.M., Kaplan, M.R., Schlüchter, C., 2010. Glacier advance in southern middle-latitudes during the Antarctic Cold Reversal. Nat. Geosci. 3, 700–704.

Reid, J.R., 1969. Effects of a debris-slide on "Sioux Glacier", South-central Alaska. J. Glaciol. 8, 353–367.

Reznichenko, N., Davies, T.R.H., Shulmeister, J., McSaveney, M.J., 2010. Effects of debris on ice-surface melting rates: an experimental study. J. Glaciol. 56, 384–394.

Reznichenko, N., Davies, T.R.H., Alexander, D.J., 2011. Effects of rock avalanches on glaciers behaviour and moraines formation. Geomorphology 132, 327–338.

Reznichenko, N.V., Davies, T.R.H., Shulmeister, J.P., Larsen, S.H., 2012. A new technique for identifying rock avalanche-sourced sediment in moraines and some palaeoclimatic implications. Geology 40, 319–322.

Robinson, T.R., Davies, T.R.H., Reznichenko, N.V., De Pascale, G.P., 2014. The extremely long-runout Komansu rock avalanche in the Trans Alai range. Pamir Mountains, southern Kyrgyzstan. Landslides. http://dx.doi.org/10.1007/s10346-014-0492-y.

Sacco, F., 1918. I ghiacciai italiani del gruppo del Monte Bianco. Boll. Com. Glaciol. Ital. 3, 21–102.

de Saussure, H.-B., 1786. Voyages dans les Alpes, précédés d'un essai sur l'histoire naturelle des environs de Genève, vol. 2. Barde, Manguet et Compagnie, Genève. XVI–641 pp.

Schneider, D., Kaitna, R., Dietrich, W.E., Hsu, L., Huggel, C., McArdell, B.W., 2011a. Frictional behavior of granular gravel-ice mixtures in vertically rotating drum experiments and implications for rock-ice avalanches. Cold Reg. Sci. Technol. 69, 70–90.

Schneider, D., Huggel, C., Haeberli, W., Kaitna, R., 2011b. Unravelling driving factors for large rock-ice avalanche mobility. Earth Surf. Processes Landforms 36, 1948–1966.

Schwab, J.W., 2002. In: Catastrophic Rock Avalanche: Howson Range, Telkwa Pass. Forest Sciences, Prince Rupert Forest Region, Extension Note, vol. 46, 5 pp.

Scott, K.M., Vallance, J.W., 1995. Debris Flow, Debris Avalanche, and Flood Hazards at and Downstream from Mount Rainier. Hydrologic Investigations Atlas (USGS), HA-729, Washington, 9 pp.

Selby, M.J., 1993. Hillslope Materials and Processes. Oxford University Press, Oxford, 451 pp.

Sharp, M., 1988. Surging glaciers; geomorphic effects. Prog. Phys. Geogr. 12, 9015–9022.

Shreve, R.L., 1968. Sherman landslide. In: The Great Alaska Earthquake of 1964 (Hydrology, Part A), Publication 1603. National Academy of Sciences, Washington, D.C, pp. 395–401.

Shugar, D.H., Clague, J.J., 2011. The sedimentology and geomorphology of rock avalanche deposits on glaciers. Sedimentology 58, 1762–1783.

Shugar, D.H., Rabus, B.T., Clague, J.J., 2010. Elevation changes (1949–1995) of Black Rapids Glacier, Alaska, derived from a multi-baseline InSAR DEM and historical maps. J. Glaciol. 56, 625–634.

Shugar, D.H., Clague, J.J., Giardino, M., 2013a. A quantitative assessment of the sedimentology and geomorphology of rock avalanche deposits. In: Margottini, C., Catani, F., Trigila, A.,

Iadanza, C. (Eds.), Landslide Science and Practice, Global Environmental Change, vol. 4. Springer-Verlag, pp. 321–326.

Shugar, D.H., Clague, J.J., McSaveney, M.J., August 2013b. Late Holocene Behavior of Sheridan and Sherman Glaciers, Chugach Mountains, Alaska. Canadian Quaternary Association. Edmonton, Canada.

Shugar, D.H., Rabus, B.T., Clague, J.J., Capps, D.M., 2012. The response of Black Rapids Glacier, Alaska, to the Denali earthquake rock avalanches. J. Geophys. Res. 117. http://dx.doi.org/10.1029/2011jf002011.

Shulmeister, J., Davies, T.R., Evans, D.J.A., Hyatt, O.M., Tovar, D.S., 2009. Catastrophic landslides, glacier behaviour and moraine formation – a view from an active plate margin. Quat. Sci. Rev. 28, 1085–1096.

Shulmeister, J., Davies, T.R.H., Reznichenko, N., Alexander, D.J., 2010. Comment on "Glacial advance and stagnation caused by rock avalanches" by Vacco, D.A., Alley, R.B. and Pollard, D. Earth Planet. Sci. Lett. 297, 700–701.

Sosio, R., Crosta, G.B., Hungr, O., 2008. Complete dynamic calibration for the Thurwieser rock avalanche (Italian Central Alps). Eng. Geol. 100, 11–26.

Sosio, R., Crosta, G.B., Chen, J.H., Hungr, O., 2012. Modelling rock avalanche propagation onto glaciers. Quat. Sci. Rev. 47, 23–40.

Strom, A., 2006. Morphology and internal structure of rockslides and rock avalanches: grounds and constraints for their modeling. In: Evans, S.G., Scarascia Mugnozza, G., Strom, A., Hermanns, R.L. (Eds.), Landslides from Massive Rock Slope Failure, NATO Science Series IV, Earth and Environmental Sciences, 49. Springer, Dordrecht, pp. 305–326.

Tovar, D.S., Shulmeister, J., Davies, T.R., 2008. Evidence for a landslide origin of New Zealand's Waiho Loop moraine. Nat. Geosci. 1, 524–526.

Uhlmann, M., Korup, O., Huggel, C., Fischer, L., Kargel, J.S., 2013. Supra-glacial deposition and flux of catastrophic rock-slope failure debris, south-central Alaska. Earth Surf. Processes Landforms 38, 675–682.

Vacco, D.A., Alley, R.B., Pollard, D., 2010. Glacial advance and stagnation caused by rock avalanches. Earth Planet. Sci. Lett. 294, 123–130.

Valbusa, U., 1924. Il ghiacciaio della Brenva (M. Bianco) dal 20 Aprile 1923 al 15 Giugnio 1924. Riv. Club Alp. Ital. 43, 270–281.

Vincent, C., Six, D., Berthier, E., Le Meur, E., 2012. Ecoulement et fluctuations de la Mer de Glace. In: Deline, P., Nussbaumer, S., Vincent, C., Zumbuhl, H. (Eds.), La Mer de Glace, art et science. Esope, Chamonix, 192 pp.

Virgilio, F., 1883. Sui recenti studi circa le variazione periodiche dei ghiacciai. Boll. Club Alp. Ital. 50, 50–70.

Voight, B. (Ed.), 1978. Rockslides and Avalanches, 1. Natural Phenomena. Elsevier, Amsterdam, 843 pp.

Wardle, P., 1978. Further radiocarbon dates from Westland National Park and the Omoeroa River mouth, New Zealand. N. Z. J. Bot. 11, 349–388.

Wegmann, M., Gudmundsson, G.H., Haeberli, W., 1998. Permafrost changes in rock walls and the retreat of alpine glaciers: a thermal modelling approach. Permafrost Periglac. 9, 23–33.

Whalley, W.B., 1984. Rockfalls. In: Brunsden, D., Prior, D.B. (Eds.), Slope Instability. Wiley, Chichester, pp. 217–256.

Zienert, A., 1965. Gran Paradiso-Mont Blanc. Prähistorische und historische Gletscherstände. Eiszeitalter Ggw. 16, 202–225.